



NAVAL POSTGRADUATE SCHOOL

MONTEREY, CALIFORNIA

THESIS

**LONG-RANGE FORECASTING IN SUPPORT
OF OPERATIONS IN PAKISTAN**

by

Jeremy A. DeHart

March 2011

Thesis Co-Advisors:

Tom Murphree
David Meyer

Approved for public release; distribution is unlimited

THIS PAGE INTENTIONALLY LEFT BLANK

REPORT DOCUMENTATION PAGE
Form Approved OMB No. 0704-0188

Public reporting burden for this collection of information is estimated to average 1 hour per response, including the time for reviewing instruction, searching existing data sources, gathering and maintaining the data needed, and completing and reviewing the collection of information. Send comments regarding this burden estimate or any other aspect of this collection of information, including suggestions for reducing this burden, to Washington Headquarters Services, Directorate for Information Operations and Reports, 1215 Jefferson Davis Highway, Suite 1204, Arlington, VA 22202-4302, and to the Office of Management and Budget, Paperwork Reduction Project (0704-0188) Washington DC 20503.

1. AGENCY USE ONLY (Leave blank)	2. REPORT DATE March 2011	3. REPORT TYPE AND DATES COVERED Master's Thesis
4. TITLE AND SUBTITLE Long-Range Forecasting in Support of Operations in Pakistan		5. FUNDING NUMBERS
6. AUTHOR(S) Jeremy A. DeHart		
7. PERFORMING ORGANIZATION NAME(S) AND ADDRESS(ES) Naval Postgraduate School Monterey, CA 93943-5000		8. PERFORMING ORGANIZATION REPORT NUMBER
9. SPONSORING /MONITORING AGENCY NAME(S) AND ADDRESS(ES) N/A		10. SPONSORING/MONITORING AGENCY REPORT NUMBER
11. SUPPLEMENTARY NOTES The views expressed in this thesis are those of the author and do not reflect the official policy or position of the Department of Defense or the U.S. Government. IRB Protocol number <u> </u> N.A <u> </u> .		
12a. DISTRIBUTION / AVAILABILITY STATEMENT Approved for public release; distribution is unlimited		12b. DISTRIBUTION CODE

13. ABSTRACT (maximum 200 words)

Skillful long-range forecasts (LRFs; lead times of several weeks or longer) are a critical component of mission planning for both military and nonmilitary operations. This is especially true for countries that are susceptible to persistent climate variations, such as Pakistan. The environmental, economic, and political impacts of climate variations can be severe—particularly for countries that are economically and politically unstable, or at risk of such instability. The United States (U.S.) has characterized stability in Pakistan as a priority for U.S. national security.

These considerations led us to investigate the potential for skillful LRFs of climate variations in Pakistan summer precipitation. These variations can lead to floods and droughts, and major economic impacts, as demonstrated by, for example, the extreme flooding in the summer of 2010. In this study, we developed methods for long-range forecasting of Pakistan precipitation during the main precipitation period of July–August. We investigated the correlations between regional and global scale climate variables and Pakistan precipitation to identify the processes associated with extreme summer precipitation events in Pakistan.

From these correlations, we identified a set of 850 hecto-Pascal (hPa) geopotential heights (GPH) in the region surrounding Pakistan as a potentially skillful predictor. We developed several LRF approaches based on this predictor and linear regression, tercile matching, and optimal climate normal methods. We tested these approaches by conducting independent hindcasts for the 41-year period of 1970–2010, and found good skill in predicting above and below normal precipitation events. We also determined that using sea surface temperatures (SSTs) as a predictor of the 850 hPa heights has the potential to provide skillful LRFs of Pakistan July–August precipitation at lead times out to six months or longer. We propose that additional research be conducted using statistical and statistical-dynamical forecast methods to develop and validate a long-range forecasting system for operational use.

14. SUBJECT TERMS Pakistan, Southwest Asia, SWA, Precipitation, Precipitation Rate, Long-range Forecasting, Climate, Climate Analysis, Climate Variations, Climate Forecasting, Climate Prediction, Teleconnections, Reanalysis, Statistical Forecast, Statistical-Dynamical Forecasting, Meteorology, Smart Climatology			15. NUMBER OF PAGES 107
			16. PRICE CODE
17. SECURITY CLASSIFICATION OF REPORT Unclassified	18. SECURITY CLASSIFICATION OF THIS PAGE Unclassified	19. SECURITY CLASSIFICATION OF ABSTRACT Unclassified	20. LIMITATION OF ABSTRACT UU

THIS PAGE INTENTIONALLY LEFT BLANK

Approved for public release; distribution is unlimited

**LONG-RANGE FORECASTING IN SUPPORT OF OPERATIONS IN
PAKISTAN**

Jeremy A. DeHart
Captain, United States Air Force
B.S., North Carolina State University, 2004

Submitted in partial fulfillment of the
requirements for the degree of

MASTER OF SCIENCE IN METEOROLOGY

from the

NAVAL POSTGRADUATE SCHOOL
March 2011

Author: Jeremy A. DeHart

Approved by: Tom Murphree
Thesis Co-Advisor

David Meyer
Thesis Co-Advisor

Philip Durkee
Chair, Department of Meteorology

THIS PAGE INTENTIONALLY LEFT BLANK

ABSTRACT

Skillful long-range forecasts (LRFs; leads times of several weeks or longer) are a critical component of mission planning for both military and nonmilitary operations. This is especially true for countries that are susceptible to persistent climate variations, such as Pakistan. The environmental, economic, and political impacts of climate variations can be severe—particularly for countries that are economically and politically unstable, or at risk of such instability. The United States (U.S.) has characterized stability in Pakistan as a priority for U.S. national security.

These considerations led us to investigate the potential for skillful LRFs of climate variations in Pakistan summer precipitation. These variations can lead to floods and droughts, and major economic impacts, as demonstrated by, for example, the extreme flooding in the summer of 2010. In this study, we developed methods for long-range forecasting of Pakistan precipitation during the main precipitation period of July–August. We investigated the correlations between regional and global scale climate variables and Pakistan precipitation to identify the processes associated with extreme summer precipitation events in Pakistan.

From these correlations, we identified a set of 850 hecto-Pascal (hPa) geopotential heights (GPH) in the region surrounding Pakistan as a potentially skillful predictor. We developed several LRF approaches based on this predictor and linear regression, tercile matching, and optimal climate normal methods. We tested these approaches by conducting independent hindcasts for the 41-year period of 1970–2010, and found good skill in predicting above and below normal precipitation events. We also determined that using sea surface temperatures (SSTs) as a predictor of the 850 hPa heights has the potential to provide skillful

LRFs of Pakistan July-August precipitation at lead times out to six months or longer. We propose that additional research be conducted using statistical and statistical-dynamical forecast methods to develop and validate a long-range forecasting system for operational use.

TABLE OF CONTENTS

I.	INTRODUCTION.....	1
	A. BACKGROUND	1
	B. PAKISTAN CLIMATE SYSTEM.....	3
	1. Geography	3
	2. Long-Term Mean Climate.....	5
	a. <i>July-August Focus</i>	6
	C. CLIMATE VARIATIONS AND IMPACTS ON PAKISTAN.....	10
	D. OPERATIONAL CLIMATE PRODUCTS FOR PAKISTAN.....	12
	1. DoD Products.....	12
	a. <i>28 Operational Weather Squadron</i>	12
	b. <i>14 Weather Squadron</i>	12
	2. Non-DoD Products.....	13
	a. <i>U.S. Products</i>	13
	b. <i>Non-U.S. Products</i>	15
	E. MOTIVATION AND SCOPE OF THIS STUDY	15
	1. Geopolitics and National Security.....	15
	2. Military Operations	16
	3. Air Force Weather Operations	18
	4. Advanced Climate Analysis and Long-Range Forecasting in DoD.....	18
	5. Research Questions	20
II.	DATA AND METHODS.....	21
	A. DATASETS AND SOURCES.....	21
	1. NCEP/NCAR Atmospheric Reanalysis.....	21
	2. Multivariate ENSO Index (MEI).....	22
	3. North Atlantic Oscillation (NAO)	22
	4. Indian Ocean Dipole Mode Index (DMI).....	22
	B. CLIMATE ANALYSIS AND FORECASTING METHODS.....	23
	1. Predictand Selection	23
	2. Composites, Correlations, and Teleconnections.....	24
	3. Predictor Selection	25
	4. Predictor and Predictand Time Series	25
	5. Long-Range Forecast Method Development and Hindcast Testing.....	26
	a. <i>Linear Regression</i>	26
	b. <i>Tercile Matching</i>	27
	c. <i>Hindcast Verification Methods</i>	28
	d. <i>Optimal Climate Normals</i>	30
	6. Forecast Systems Development.....	31
	C. SUMMARY OF CLIMATE ANALYSIS AND FORECASTING METHODS	31

III. RESULTS	33
A. CLIMATE ANALYSIS RESULTS.....	33
1. Predictand Selection	33
2. Composite Analysis	37
a. <i>Long-Term Means</i>	37
b. <i>Conditional Anomalies</i>	40
3. Correlations and Teleconnections	44
4. Predictor Selection	48
a. <i>Initial Predictors</i>	48
b. <i>Final Predictors and Pakistan Summer Precipitation Index (PSPI)</i>	50
5. Predictor and Predictand Time Series	51
B. LONG-RANGE HINDCAST RESULTS.....	52
1. Linear Regression	52
2. Tercile Matching	56
3. Hindcast Verification Results	58
4. Optimal Climate Normals	59
C. POTENTIAL LONG-RANGE FORECAST SYSTEMS	64
1. Direct Statistical Approach	65
2. Direct Dynamical Approach.....	67
3. Statistical-Dynamical Approach	69
IV. CONCLUSION AND RECOMMENDATIONS	73
A. SUMMARY AND KEY RESULTS	73
B. RECOMMENDATIONS FOR FUTURE RESEARCH.....	75
LIST OF REFERENCES.....	77
INITIAL DISTRIBUTION LIST	83

LIST OF FIGURES

Figure 1.	Map of Southwest Asia. The red box overlays Pakistan.....	4
Figure 2.	Physical relief map of Pakistan and surrounding countries. Elevation changes are extreme between the high peaks of the Hindu Kush mountains in the north, and the Thar Desert in the south. (“Pakistan Topography,” after Wikipedia 2010; available online at: http://upload.wikimedia.org/.../Pakistan_Topo...) ...	5
Figure 3.	Monthly precipitation rate (PR; mm/day; dark blue bars) and standard deviation of the PR (SD; mm/day; light blue bars) in central Pakistan (27° – 32° N, 67° – 75° E). The Jul–Aug period falls during the southwest monsoon, which occurs from June–September. The PR during Jul–Aug is clearly the highest of the year in both intensity and SD. The high Jul–Aug PR and variability make this a particularly important variable to predict at long lead times. Thus, we chose Jul–Aug PR in Pakistan as our primary long-range forecasting (LRF) target, or predictand, for the LRFs we developed and tested in this study. PR data from global reanalysis data set described in Chapter II, Section A.1.	7
Figure 4.	LTM composite of surface PR (mm/day) during Jul–Aug for 1970–2010. Jul–Aug is a period of relatively high precipitation for Pakistan (see Figure 3). Pakistan precipitation in this period is: (1) highest in the northern half of the country where there is higher terrain (see Figure 2); and (2) less than in south Asian nations further to the east but higher than in Southwest Asia (SWA). PR data from global reanalysis data set described in Chapter II, Section A.1.	8
Figure 5.	(a) Schematic low level circulation during the summer southwest monsoon (from Danielson et al. 2003). Low pressure over south Asia forces a moist, onshore flow from the Indian Ocean leading to heavy rainfall (see Figures 3–4). (b) Surface vector winds (m/s) for June–July–August–September (JJAS; from Kripalani 2007). The Somali jet is evident as it flows northeastward along the east coast of Africa and the Arabian Peninsula and across the Arabian Sea. The blue arrow represents a branch of the Somali Jet that provides Pakistan with a relatively high PR during the JJAS.	9
Figure 6.	LTM composite of 850 hPa GPH (m) for Jul–Aug. Note the low heights from Pakistan through southern China, which leads to the circulation and precipitation patterns described in Figures 3–5. PR data from the global reanalysis data set described in Chapter II, Section A.1.	10
Figure 7.	Time series of Jul–Sep surface temperature ($^{\circ}$ C) in Iraq from 1968–2005. The solid and dashed blue lines represent the long-term mean surface temperature and long-term mean range, which are	

the basis for the traditional climatology approaches typically used by DoD in providing climate support. The solid red line and red ovals highlight the interannual and long-term trend in the surface temperature, which are examples of the additional types of climate information that are exploited when using smart climatology approaches to provide climate support. (From Murphree 2010a).....	19
Figure 8. Flow chart showing main datasets and methods used to conduct climate analyses and long-range forecasts in this study and recommendations for future studies. (Adapted from Lemke 2010)	32
Figure 9. Physical relief map of Pakistan overlaid with the three predictand regions considered in this study. The coordinates for the predictand regions are: (a) Box 1: 27°–32°N, 67°–75°E; (b) Box 2: 32°–35°N, 70°–75°E; and (c) Box 3: 30°–33°N, 67°–69°E. After conducting the analysis methods described in Chapter II, Section B, we ultimately chose Box 2 (outlined in yellow) as our main predictand region. (“Pakistan Topography,” after Wikipedia 2010; available online at: http://upload.wikimedia.org/.../Pakistan_Topography.png)	34
Figure 10. (a) Jul–Aug LTM PR (mm/day); and (b) Jul–Aug 2000–2010 PR anomaly (mm/day). The predictand boxes considered for this study are overlaid. We initially chose each box as a potential predictand after analyzing annual PR patterns from 1970–2010. Ultimately, we selected Box 2 after considering: (1) the LTM PR amounts and variations; (2) the 2000–2010 PR amounts and variations; and (3) the impact to flooding. Thus, all references to Pakistan PR throughout the remainder of this study refer to the Box 2 predictand region.	35
Figure 11. Time series of Jul–Aug Pakistan PR (mm/day) from 1970–2010. Note the uptrend of 0.35 mm/day per decade since 1970, and the spike in 2010 associated with the record flooding described in Chapter I, Section A.	37
Figure 12. Jul–Aug LTM: (a) PR (mm/day); (b) 200 hPa GPH (m); (c) 850 hPa vector winds (m/s); and (d) 850 hPa GPH (m). Jul–Aug is characterized by a strong lower tropospheric trough over southern Asia (d) that is overlain by a strong upper tropospheric ridge (b). This height pattern allows for a northern branch of the Somali jet (red arrow in c, d) to bring moisture from the Arabian Sea into Pakistan (c, d) leading to high PR over much of southern Asia, with Pakistan lying just to the west of this high precipitation region.	38
Figure 13. Jul–Aug LTM: (a) PR (mm/day); (b) OLR (W/m ²); (c) 850 hPa specific humidity (g/kg); and (d) 700 hPa omega (Pa/s). As expected, high PR (a) tends to be associated with low OLR (b), high 850 hPa specific humidity (c), and upward vertical motion (d). Pakistan lies on the western (eastern) edge of the region in which	

conditions are favorable (unfavorable) for high PR (cf. Figures 12–13).	39
Figure 14. Conditional composite anomalies of PR (mm/day) for the eight most extreme wet (left panel) and dry (right panel) Pakistan PR events during Jul–Aug 1970–2010. The red boxes outline our predictand region. Note the isolation of the anomalies to the north-central portion of Pakistan, in and close to the predictand region.	41
Figure 15. Conditional composite anomalies of SST (°C) for the eight most extreme wet (left panel) and dry (right panel) Pakistan PR events during Jul–Aug 1970–2010. Note the general absence of strong clear patterns in either wet or dry year composites. This indicates that SST may not be a good direct predictor of Pakistan PR.	41
Figure 16. Conditional composite anomalies of 850 hPa GPH (m) for the eight most extreme wet (left panel) and dry (right panel) Pakistan PR events during Jul–Aug 1970–2010. The red arrows schematically represent the corresponding wind anomalies that are likely to affect Pakistan. Note in the wet (dry) composite the anomalous high (low) over the Nepal region providing a moist easterly (dry westerly) flow into Pakistan. Low-level convergent (divergent) flow also characterizes wet (dry) years over and near Pakistan.	42
Figure 17. Conditional composite anomalies of 700 hPa omega (Pa/s) for the eight most extreme wet (left panel) and dry (right panel) Pakistan PR events during Jul–Aug 1970–2010. The red boxes outline our predictand region. Note in the wet (dry) composite the negative (positive) anomalies over Pakistan indicating an increase (decrease) in upward vertical motion.	43
Figure 18. Conditional composite anomalies of 850 hPa specific humidity (g/kg) for the eight most extreme wet (left panel) and dry (right panel) Pakistan PR events during Jul–Aug 1970–2010. The red boxes outline our predictand region.	44
Figure 19. Correlation of Pakistan PR (mm/day) for Jul–Aug 1970–2010 with regional 850 hPa GPH (m) at zero lead. Note the strong positive correlation in the Nepal region, weak positive correlation in the Caspian Sea region, and strong negative correlation in the Red Sea region.	46
Figure 20. Schematic of 850 hPa GPH anomalies and OLR anomalies for extreme wet (top panel) and dry (lower panel) Pakistan PR events during Jul–Aug 1970–2010. Note during wet (dry) years, the teleconnection of AN (BN) convection near the maritime continent in May–June with higher (lower) tropospheric heights near Nepal in Jul–Aug, indicating a two-month lead teleconnection. Figures based on conditional composite anomaly and correlation results (cf. Figures 14–19).	47
Figure 21. Correlation of Pakistan PR in Jul–Aug with regional 850 hPa GPH for (a) 1970–2010; and (b) 2000–2010. Strong zero lead	

correlations between Pakistan PR and 850 hPa GPH led to using 850 hPa GPH as our main initial predictor. The red boxes in (a) and/or (b) outline the regions where we observed the strongest correlations. We selected the regions enclosed by these five boxes as our initial predictor regions. These boxes are referred to in this study as (from west to east): Red Sea box (12° – 20° N, 35° – 47° E), Caspian box (35° – 45° N, 45° – 55° E), Afghan box (28° – 33° N, 75° – 85° E), Nepal West box, and Nepal East box (25° – 30° N, 85° – 100° E). 49

Figure 22. Correlation of Pakistan PR in Jul–Aug with global 850 hPa GPH for (a) 1970–2010; and (b) 2000–2010. This is a duplicate of Figure 21 but with the 850 hPa GPH regions used in the Pakistan Summer Precipitation Index (PSPI) outlined in red and the eliminated predictor regions outlined in gray. The red boxes are the Red Sea box and the Nepal West box (see latitude and longitude ranges in Figure 21). 51

Figure 23. Time series of 1970–2010 Jul–Aug Pakistan PR as observed (mm/day; gray line) and as modeled by the Pakistan Summer Precipitation Index (PSPI, m; blue line). The correlation between the two time series is 0.694, which is statistically significant at a $> 99\%$ confidence level. Note that the PSPI provides a good representation of many of the interannual variations, and of the long-term upward trend, in the Pakistan PR. These results indicate that the PSPI is a high potential to be a skillful zero lead predictor of Pakistan PR. 52

Figure 24. Mean 850 hPa GPH (m) for Jul–Aug 1970–1999 (left panel) and 2000–2010 (right panel). The red boxes represent the boundaries of our initial predictors (see Chapter III, Section A.4.a). Note that mean 850 hPa GPH was relatively high across much of west Asia (e.g., near the Caspian Sea) during 2000–2010. This could be a cause of the changing correlation pattern between Pakistan PR and 850 hPa GPH when comparing the same periods (see Figure 21). ... 60

Figure 25. Correlation for 1970–2010 of May–Jun SST with the subsequent Jul–Aug: (a) Pakistan PR; and (b) PSPI (two-month lead correlations). Panel (a) shows a generally weak relationship between SST and Pakistan PR. Panel (b) shows strong relationships between SST and Pakistan PR, and thus indicates a high potential for developing a direct two-step statistical model using SST to produce a non-zero lead forecast of PSPI, and then using this forecasted PSPI to forecast Pakistan PR. 66

Figure 26. Correlation for 1970–2010 of May–Jun SST with the subsequent Jul–Aug 850 hPa GPH in the: (a) Nepal West region; and (b) Red Sea region (two-month lead correlations). Panels (a) and (b) show strong large scale relationships between SST and the GPH predictor regions. The Nepal GPH appears to have a strong link to

SSTs in the tropical IO and MC region. The Red Sea GPH appears to have a strong link to ENLN events in the tropical Pacific. Both figures indicate: (a) the physical plausibility of using global scale SSTs to forecast the 850 hPa GPH variables used in the PSPI; and (b) the potential for using a two-step statistical model to forecast Jul-Aug Pakistan PR.....	67
Figure 27. NCEP CFS forecast of Aug 2010 PR at a two-month lead (mm/month, left panel) and verifying NCEP reanalysis of Aug 2010 PR (mm/day, right panel). Note that CFS did not accurately forecast the high PR anomaly over Pakistan.....	68
Figure 28. NCEP CFS forecast of Aug 2010 700 hPa GPH at a two-month lead (m, left panel) and verifying NCEP reanalysis of Aug 2010 700 hPa GPH (m, right panel). Note that CFS accurately forecasted the positive GPH anomaly over southern Asia (red oval).	69
Figure 29. Overview of a statistical-dynamical system for producing LRFs of Jul-Aug Pakistan PR. (After Murphree 2010b)	70
Figure 30. Two potential variations of the S-D approach to producing LRFs of Jul-Aug Pakistan PR. (a) At leads of 1–6 months, use a dynamical model (e.g., CFS) to predict 850 hPa GPH in Jul-Aug, then use the predicted GPH to force a regression model that predict Jul-Aug Pakistan PR. (b) At leads of 4–6 months, use a dynamical model (e.g., CFS) to predict SST at leads of 1–3 months, then use the predicted SST as the predictor in a regression of 850 hPa GPH in Jul-Aug, and then use the predicted GPH in a regression to predict Jul-Aug Pakistan PR.....	71

THIS PAGE INTENTIONALLY LEFT BLANK

LIST OF TABLES

Table 1.	Fall and winter precipitation anomalies in SWA due to climate variations (from Vorhees 2006). The pluses and minuses indicate a positive or negative phase of the climate variation, respectively.	11
Table 2.	Schematic contingency table used to verify hindcasts of Jul-Aug Pakistan PR. The cells of the table represent the number and combinations of observed occurrences (obs Y), observed non-occurrences (obs N), predicted occurrences (pred Y), and predicted non-occurrences (pred N) of Pakistan PR. A separate contingency table was used for each of the three tercile categories for Pakistan PR (AN, NN, and BN). We used the values from this table to calculate several hindcast verification metrics including accuracy rate, probability of detection (POD), false alarm rate (FAR), and Heidke skill score (HSS). (After Wilks 2006)	29
Table 3.	Correlation of initial predictors with Jul–Aug 1970–2010 Pakistan PR. Each predictor represents the 850 hPa GPH anomaly within its respective bounded region (Figure 21). The 5-Variable Index denotes a single predictor created by an equal weight combination of all five predictors. Correlations > 0.30 are considered statistically significant at a 95% confidence level.....	50
Table 4.	Multivariate linear regression results for our initial predictors (see Table 3) used to model Jul–Aug 1970–2010 Pakistan PR. Each predictor represents the 850 hPa GPH anomaly (Z850) within the regions shown in Figure 21. The multivariate index denotes a single predictor created by an equal weight combination of all five individual predictors. Correlations ≥ 0.30 , significance $F \leq 0.05$, and p-values ≤ 0.05 are considered statistically significant at a 95% confidence level.....	53
Table 5.	The three most significant multivariate regression results, ranked by adjusted R-square, for modeling of. Jul–Aug 1970–2010 Pakistan PR. Each predictor represents the 850 hPa GPH anomaly (Z850) within the regions shown in Figure 21. Each of the three multivariate indices denotes a single predictor created by combining the predictors shown just below each of the indices. Correlations ≥ 0.30 , significance $F \leq 0.05$, and p-values ≤ 0.05 are considered statistically significant at a 95% confidence level. The red outline denotes the only multivariate regression model that met each of these thresholds.	55
Table 6.	Tercile matching hindcast results when using PSPI (modeled PR index) to hindcast Pakistan PR (observed PR, mm/day), sorted by year. The years are shown in the left column and the PSPI and Pakistan PR values are shown in the two right columns.	

Table 7.	Green=AN, white=NN, red=BN. A color match between the two right columns indicates a correct hindcast.....	57
Table 8.	Tercile ranges for the results in Table 6. The tercile thresholds were selected by separating the PSPI and Pakistan PR data into thirds. Values in the highest third (middle third, lowest third) were placed in the AN (NN, BN) category.....	58
Table 9.	Contingency table hindcast verification results for tercile matching hindcasts using PSPI to hindcast Jul–Aug 1970–2010 Pakistan PR. The upper (middle, lower) sub-table represents the verification results for the AN (NN, BN) hindcasts. Four verification scores are shown to the right of each sub-table. See Chapter II, Section 5.3 and Table 2 for more information about contingency table-based verification methods.....	59
Table 10.	Multivariate regression results for Jul–Aug 2000–2010 Pakistan PR using as a predictor: (a) PSPI; and (b) a second combination of predictors to potentially replace the PSPI. Correlations ≥ 0.55 , significance $F \leq 0.05$, and p-values ≤ 0.05 are considered statistically significant at a 95% confidence level. Note in (a) that when PSPI is based on data from just 2000–2010, the Red Sea predictor has a p-value outside our thresholds. The predictors in (b) had the best regression results in modeling 2000–2010 Pakistan PR.	62
Table 11.	Contingency table hindcast verification results for tercile matching hindcasts using UPSPI to hindcast Jul–Aug 2000–2010 Pakistan PR. The upper (middle, lower) sub-table represents the verification results for the AN (NN, BN) hindcasts. Four verification scores are shown to the right of each sub-table. See Chapter II, Section 5.3 and Table 2 for more information about contingency table based verification methods.....	63
	Verification results for zero lead tercile matching hindcasts using PSPI and UPSPI to hindcast Jul–Aug Pakistan PR for 1970–2010 (left table) and 2000–2010 (right table). The upper (middle, lower) sub-table shows the verification results for the AN (NN, BN) hindcasts. Four verification scores are shown in each sub-table. See Chapter II, Section 5.3 and Table 2 for more information about contingency table based verification methods.....	64

LIST OF ACRONYMS AND ABBREVIATIONS

14 WS	14 Weather Squadron
28 OWS	28 Operational Weather Squadron
AFCCC	Air Force Combat Climatology Center
AFSOC	Air Force Special Operations Command
AFW	Air Force Weather
AFWA	Air Force Weather Agency
AN	Above normal
AOR	Area of responsibility
BN	Below normal
CENTCOM	Central Command
CFS	Climate Forecast System
CPC	Climate Prediction Center
DMI	Dipole Mode Index
DoD	Department of Defense
ECMWF	European Centre for Medium-range Weather Forecasts
EN	El Nino
ENLN	El Nino–La Nina
FOA	Field Operating Agency
g/kg	grams per kilogram
GPH	Geopotential height
HA/DR	Humanitarian aid and disaster relief
HOA	Horn of Africa
hPa	Hecto-pascal
HSS	Heidke skill score
IO	Indian Ocean
IOD	Indian Ocean Dipole
IOZM	Indian Ocean Zonal Mode
IPCC	Intergovernmental Panel on Climate Change

IRI	International Research Institute for Climate and Society
JJAS	June-July-August-September
Jul-Aug	July-August
LN	La Nina
LRF	Long-range forecast
LTM	Long-term mean
m	meter
m/s	meters per second
m^2	square meter
May-Jun	May-June
MC	Maritime continent
MEI	Multivariate ENSO Index
NAO	North Atlantic Oscillation
NAOI	North Atlantic Oscillation Index
NCAR	National Center for Atmospheric Research
NCDC	National Climatic Data Center
NCEP	National Centers for Environmental Prediction
NN	Near normal
NOAA	National Oceanographic and Atmospheric Administration
NPS	Naval Postgraduate School
OWS	Operational Weather Squadron
Pa/s	Pascals per second
PSPI	Pakistan Summer Precipitation Index
QDR	Quadrennial Defense Review
S-D	Statistical-dynamical
SOWT	Special Operations Weather Team
STOL	Short take-off and landing
U.S.	United States
UKMO	United Kingdom Meteorological Office
UN	United Nations

UPSPI	Updated Pakistan Summer Precipitation Index
USAF	U.S. Air Force
W/m ²	Watts per square meter
WS	Weather Squadron
WWA	Watches, warnings, and advisories
WXG	Weather Group

THIS PAGE INTENTIONALLY LEFT BLANK

ACKNOWLEDGMENTS

I would like to thank Dr. Tom Murphree and Mr. David Meyer for the time and energy you graciously supplied throughout this demanding, yet captivating project. I have learned so much from you in just these past few months. Your contributions and expertise were truly invaluable, and without them, this thesis would not have been possible. Thank you also to the Earth System Research Laboratory—the analysis tools on your website allowed us to conduct our research efficiently and to produce the majority of the figures seen throughout this paper.

I offer my gratitude to the Naval Postgraduate School for allowing me this unique opportunity to serve my country. Thank you especially to the faculty of the Meteorology department, and to my esteemed classmates and colleagues, who challenged me each and every day.

Thank you to my friends and family who have supported me in my educational ambitions from start to finish. In particular, I extend my sincerest appreciation to my wife, Lindsay, for your devotion and sacrifice while I focused on my studies. "An excellent wife who can find? She is more precious than jewels." (Proverbs 31:10)

Finally, Thank You to my Father in heaven for Your unmerited grace and continued faithfulness in seeing me through yet another trying time in my life. "For from Him and through Him and to Him are all things. To Him be the glory forever." (Romans 11:36)

THIS PAGE INTENTIONALLY LEFT BLANK

I. INTRODUCTION

A. BACKGROUND

Pakistan has regularly been in the global spotlight in recent decades due to political unrest, national and international security threats, and numerous natural disasters that have plagued the country (State Department Documents 2010). Most recently, severe weather events—and specifically, the linking of these events to climate change—have generated many of these headlines.

In late July of 2010, one of the most severe monsoonal rain events on record led to devastating floods in northern Pakistan. The event began on July 12, 2010, and lasted for several weeks, with ten inches of rain falling on a single day in the largest city affected. The subsequent flooding drowned 2,000 people and displaced 20 million others (or 12% of the population), while submerging 20% of Pakistan's territory, an area roughly the size of Italy (*Washington Post* 2011; *Financial Post* 2010a).

An event of this magnitude was sure to spark discussion of Pakistan's vulnerability to climate change. While R K Pachauri, chief of the United Nations' (UN) Intergovernmental Panel on Climate Change (IPCC), stipulated that it would be scientifically incorrect to link any single set of events with climate change, he said, "The floods of the kind that hit Pakistan may become more frequent and more intense in the future in this and other parts of the world" (Global Information Network 2010). In fact, Pakistan has since found itself on lists of countries that are the "most vulnerable to climate change" according to the European Union and the UN (*Financial Post* 2010a and 2010b). While funding for humanitarian aid and potential economic risk largely dictated the categorization of these particular lists, they do underscore: (a) the wide scope of detrimental impacts caused by severe weather events in Pakistan; and (b) rapidly increasing public awareness of these impacts.

The threat to global security is perhaps an even more important consideration. In the aftermath of the July 2010 floods, many desperate refugees sought aid from militant groups in the northern regions of the country, where government aid was too slow or too little. A similar reliance by refugees on militant groups occurred in the wake of the 2005 earthquake in Pakistan, leading to greater legitimacy for militant groups (Berger 2010). This phenomenon undoubtedly poses a security threat to every country with interests in the region, including the United States (U.S.; Berger 2010). In fact, the United States took an official stance on the security implications of climate change as a whole in February 2010 when the U.S. Department of Defense (DoD) released the most recent version of the Quadrennial Defense Review (QDR), a four-yearly report on the direction of national security strategy. It stated that "climate change [is a] key [issue] that will play a significant role in shaping the future security environment." The report added that "while climate change alone does not cause conflict, it may act as an accelerant of instability or conflict, placing a burden to respond on civilian institutions and militaries around the world" (U.S. DoD 2010). The U.S. Congressional Research Service wrote a separate report before these floods occurred on "security and the environment in Pakistan," which listed some ways that climate change could undermine security (Berger 2010). The potential threats included rising tensions from refugee migration and the creation of conditions that "foment extremists or terrorists." Former U.S. Senator and Secretary of the Navy John Warner later commented, "They do have a fragile governmental situation [in Pakistan] and this flood poses risks to the central government system, and this indeed affects our national security" because of the close links between the United States and Pakistan (Berger 2010).

The direct link between climate change and the 2010 flooding in Pakistan is debatable, but the implications of a severe climate variation of this magnitude in this part of the world are clear. Thus, there is a clear need for skillful long-range forecasts (LRFs; lead times of two weeks or longer) for Southwest Asia (SWA). In this particular case, the European Centre for Medium-range Weather

Forecasts (ECMWF) had predicted an 80% probability of severe rainfall 8–10 days in advance. However, the ECMWF simply does not have the resources to provide specific medium-range (or long-range) forecasts to the governments of individual nations and has stated it is not their role to do so (see Chapter I, Section D.2.b.1). Instead, ECMWF posts global weather simulations online for members of the World Meteorological Association, including Pakistan, to use as they see fit (*Washington Post* 2011). In this case, the ECMWF forecast went largely unnoticed and Pakistan was ill prepared for the massive flooding that occurred. This case exposes critical gaps in the timeliness of the production and dissemination of forecasts. It also raises the question of what could have been done to prepare for heavy precipitation at various lead times (e.g., a lead of 8–10 days, two weeks, two months, etc.).

In this study, we have investigated the potential for improving LRFs of extreme precipitation events in Pakistan. We developed and tested long-range forecasting systems in order to meet our major objectives for this study:

1. Understand the physical processes that lead to anomalous summer precipitation events in Pakistan.
2. Develop and test methods for forecasting anomalous summer precipitation events in Pakistan.
3. Develop the basic research foundation for skillful operational LRFs at the intraseasonal and longer lead times needed for effective planning by military and nonmilitary organizations.

B. PAKISTAN CLIMATE SYSTEM

1. Geography

To understand the climate system of Pakistan, we first must have a grasp of the geography. Pakistan is bordered by Iran on the west, Afghanistan on the northwest, China on the northeast, India on the east and the Arabian Sea on the south (Figures 1, 2).

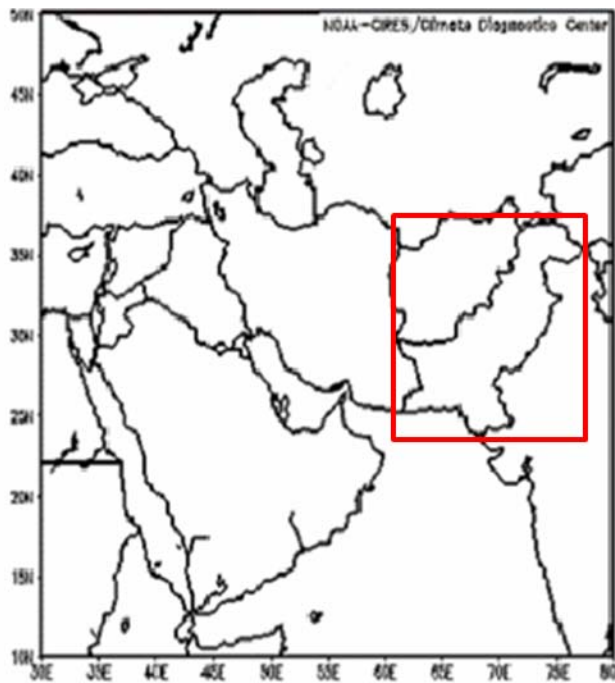


Figure 1. Map of Southwest Asia. The red box overlays Pakistan.

The total land area consists of 803,940 square kilometers (14 Weather Squadron; 14 WS 2010). Western and northern Pakistan is mountainous, while eastern Pakistan is a lowland river basin, which is commonly called the Trans-Indus basin (Figure 2). The mountains have steep, heavily forested slopes and sharp, snow-capped peaks tower to more than 25,000 feet (7,620 meters) in the Hindu Kush Mountains (14 WS 2010). Southwestern Pakistan has extensive mountain ranges, but the mountain peaks do not exceed 8,000 feet (2,500 meters). The Indus River complex meanders through the central plains and divides the northern region into three major plateaus: the Peshawar, the Potwar and the Silakot. The Indus River and its tributaries form a north-to-south oriented drainage basin, with the main river emptying into the Arabian Sea (Figure 2). The lower lying regions of Pakistan are very arid and prone to dust storms (14 WS 2010). The Thal and Thar Deserts are located in east-central Pakistan and the Kacchi Desert and Nok Kundi area lie in southwest Pakistan (14 WS 2010).

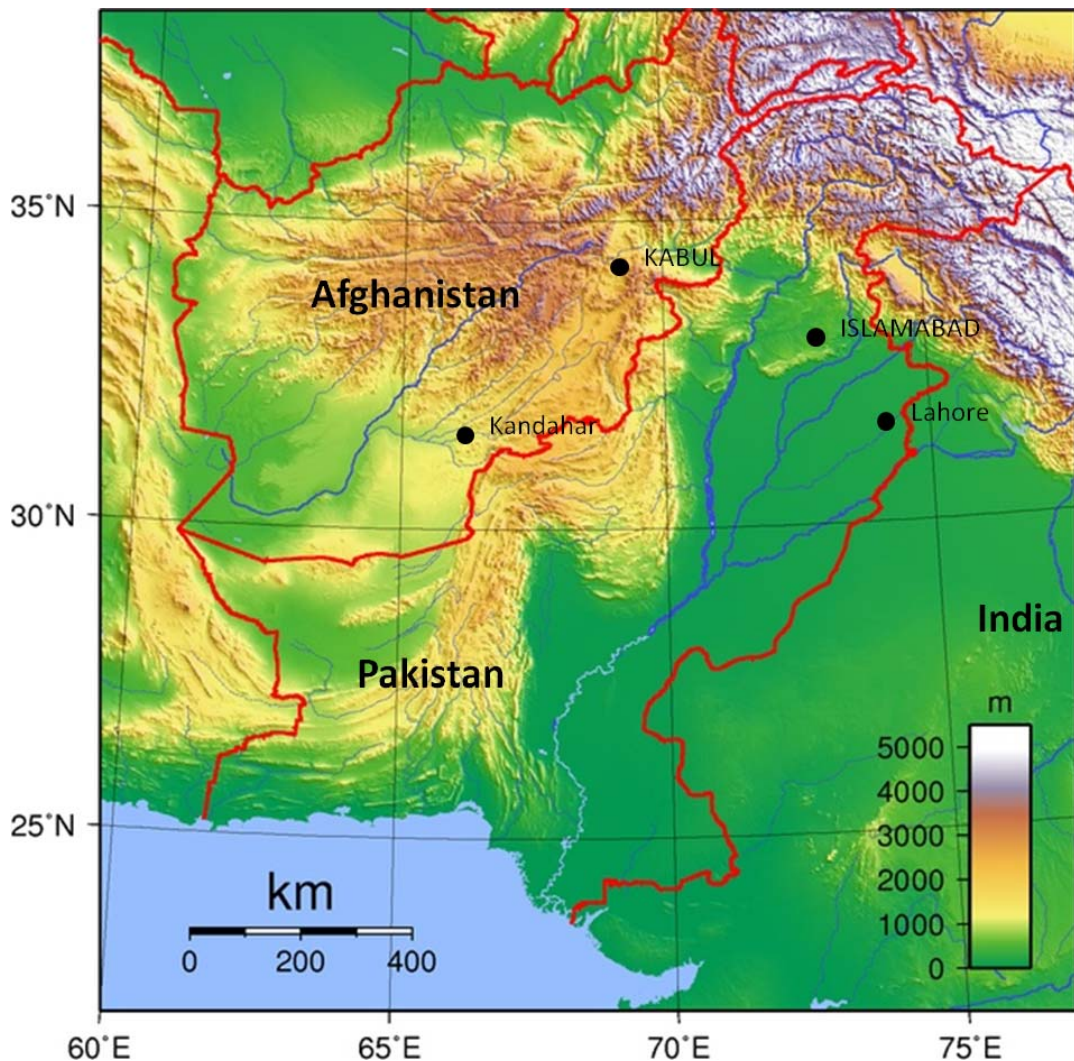


Figure 2. Physical relief map of Pakistan and surrounding countries. Elevation changes are extreme between the high peaks of the Hindu Kush mountains in the north, and the Thar Desert in the south. (“Pakistan Topography,” after Wikipedia 2010; available online at: http://upload.wikimedia.org/.../Pakistan_Topography.png)

2. Long-Term Mean Climate

Arid to semiarid conditions characterize Pakistan’s overall climate. The Indus River basin in the east and the mountains in the west and north separate the country into two distinct climate zones. The mountains, especially in the north, receive the majority of their precipitation during the northeast monsoon, which dominates the weather pattern from November–March (14 WS 2010).

North-facing slopes get the heaviest precipitation and fiercest winter weather during this time of year. The south-facing mountains and Indus basin get their brunt of the precipitation during the southwest monsoon, which runs from June through early September (14 WS 2010). See Vorhees (2006) and narratives issued by the 14 WS for more information on the climate regimes of SWA and Pakistan.

a. *July-August Focus*

To meet our objectives for this study (see Chapter I, Section A), we needed to select a focus period that gave us the best opportunity for studying anomalous precipitation events in Pakistan. Figure 3 shows the monthly annual long-term mean (LTM) precipitation rate (PR) from 1970–2010 for an area representative of the majority of the Indus River basin. Notice that the majority of the precipitation falls during July-August (Jul-Aug). Jul-Aug is also the period with the highest standard deviation in PR, indicating high variability (large, frequent anomalies) in the amounts of interannual precipitation. For these reasons, we chose Jul-Aug as our focus period.

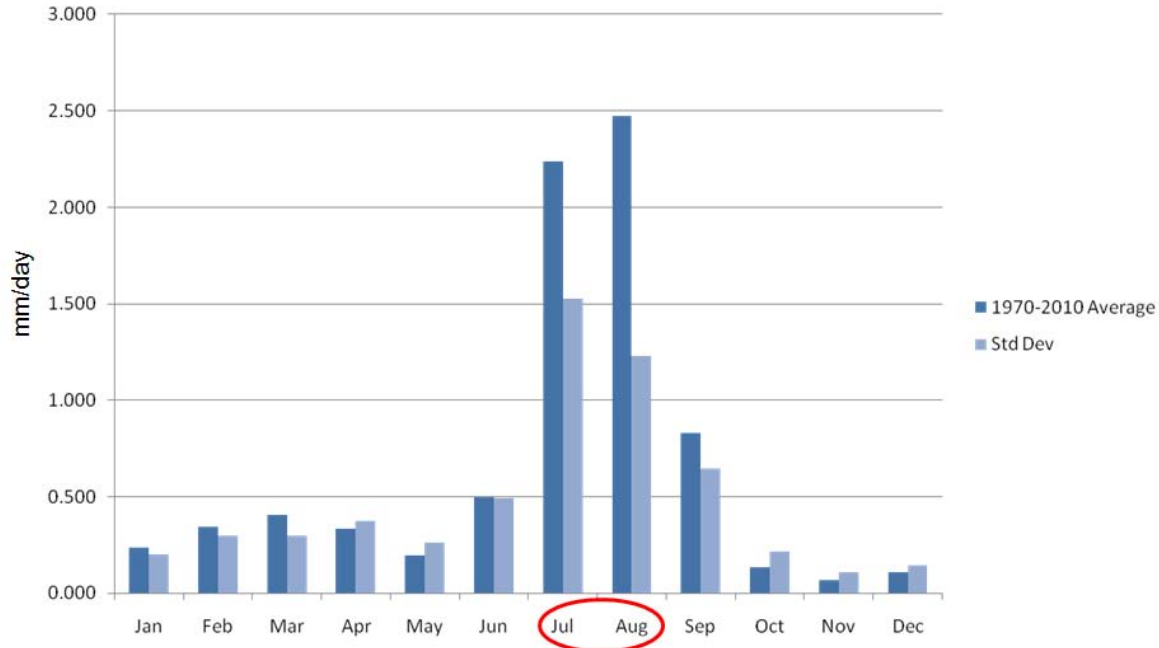


Figure 3. Monthly precipitation rate (PR; mm/day; dark blue bars) and standard deviation of the PR (SD; mm/day; light blue bars) in central Pakistan (27° – 32° N, 67° – 75° E). The Jul–Aug period falls during the southwest monsoon, which occurs from June–September. The PR during Jul–Aug is clearly the highest of the year in both intensity and SD. The high Jul-Aug PR and variability make this a particularly important variable to predict at long lead times. Thus, we chose Jul–Aug PR in Pakistan as our primary long-range forecasting (LRF) target, or predictand, for the LRFs we developed and tested in this study. PR data from global reanalysis data set described in Chapter II, Section A.1.

Figure 4 shows the spatial distribution of PR during our Jul-Aug focus period. Notice that Pakistan essentially separates the extremely wet south Asian region from the arid SWA region. While Jul-Aug is the wettest period of the year for the majority of Pakistan, this is especially the case for the south-facing mountains as noted in Chapter I, Section 2. A comparison of Figure 2 and Figure 4 indicates that the highest PR totals are along the slopes and foothills of these mountains.

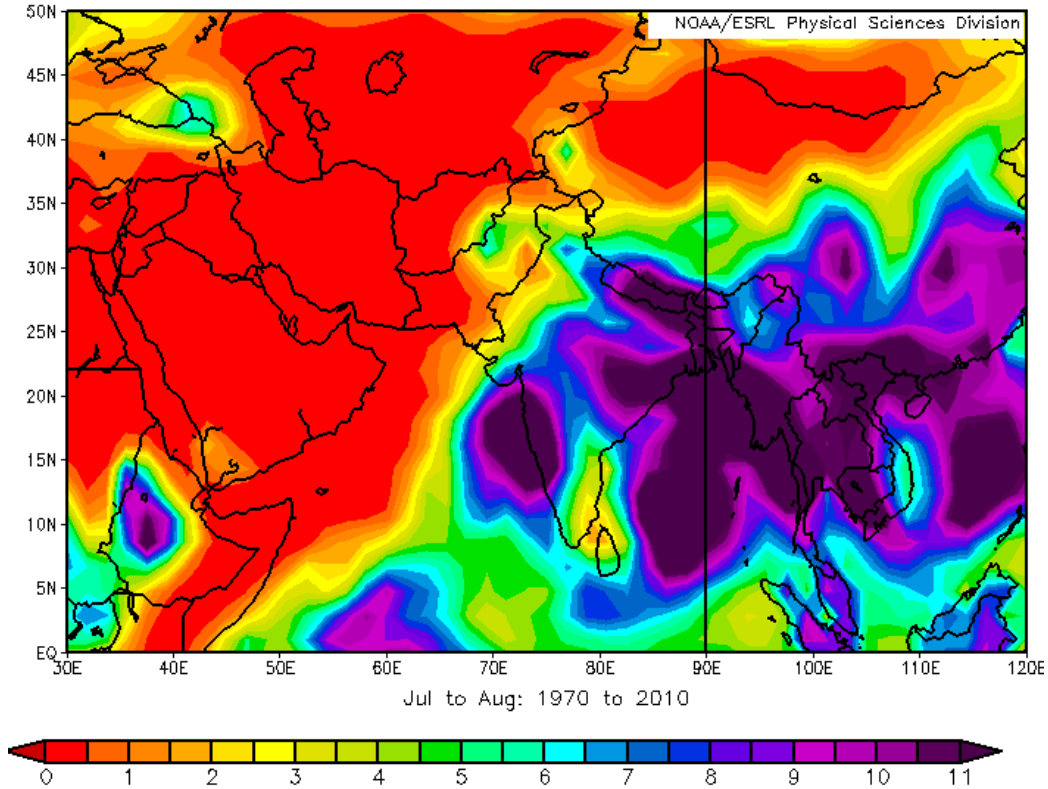


Figure 4. LTM composite of surface PR (mm/day) during Jul–Aug for 1970–2010. Jul–Aug is a period of relatively high precipitation for Pakistan (see Figure 3). Pakistan precipitation in this period is: (1) highest in the northern half of the country where there is higher terrain (see Figure 2); and (2) less than in south Asian nations further to the east but higher than in Southwest Asia (SWA). PR data from global reanalysis data set described in Chapter II, Section A.1.

As noted in Chapter I, Section 2, the southwest monsoon is responsible for the influx of moisture into Pakistan during Jul-Aug. Figure 5a gives a schematic graphical description of the lower tropospheric circulation that drives this moisture influx. Note a broad area of low heights from SWA eastward through southern China. The surface wind vectors in Figure 5b give a more thorough illustration of the resulting flow. The Somali jet is the predominant feature in this figure, as it flows northeastward over the northwestern Indian Ocean (IO) and Arabian Sea. A northern branch of the Somali jet (blue arrow in Figure 5b) brings warm, moist air into Pakistan.

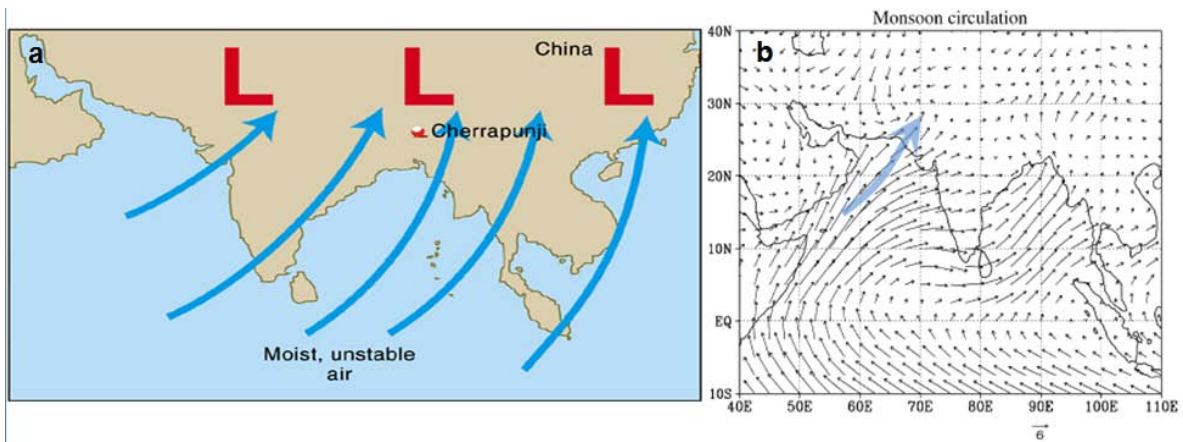


Figure 5. (a) Schematic low level circulation during the summer southwest monsoon (from Danielson et al. 2003). Low pressure over south Asia forces a moist, onshore flow from the Indian Ocean leading to heavy rainfall (see Figures 3–4). (b) Surface vector winds (m/s) for June-July-August-September (JJAS; from Kripalani 2007). The Somali jet is evident as it flows northeastward along the east coast of Africa and the Arabian Peninsula and across the Arabian Sea. The blue arrow represents a branch of the Somali Jet that provides Pakistan with a relatively high PR during the JJAS.

A map of the Jul-Aug LTM 850 hecto-Pascal (hPa) geopotential height (GPH) shows a pronounced trough across southern Asia, from SWA to southern China (Figure 6). The most prominent feature of this thermally-induced trough is the Pakistani Heat Low (14 WS 2010) that forces the low-level flow into convergence over Pakistan, which characterizes the southwest monsoon during JJAS (cf. Vorhees 2006; 14 WS 2010).

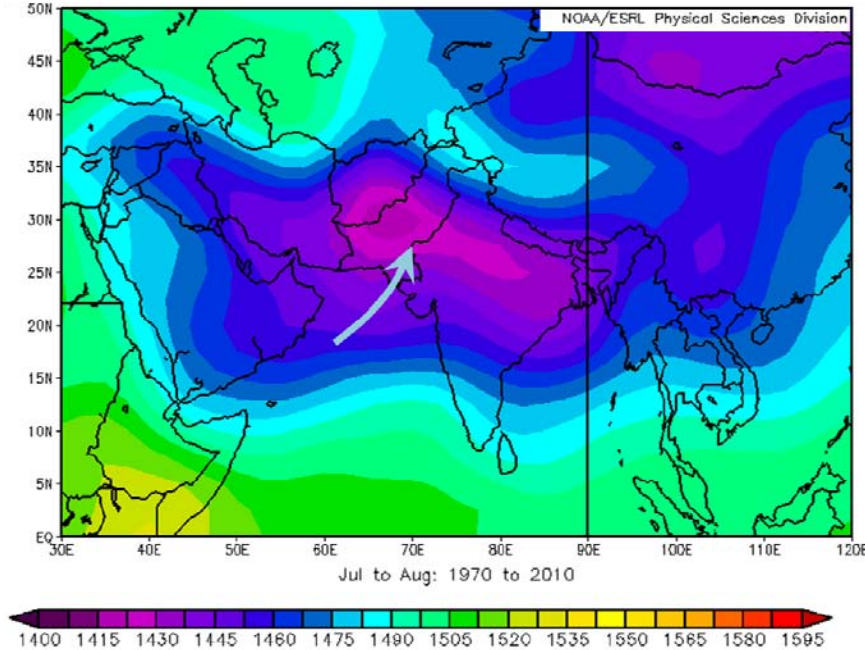


Figure 6. LTM composite of 850 hPa GPH (m) for Jul–Aug. Note the low heights from Pakistan through southern China, which leads to the circulation and precipitation patterns described in Figures 3–5. PR data from the global reanalysis data set described in Chapter II, Section A.1.

C. CLIMATE VARIATIONS AND IMPACTS ON PAKISTAN

A *teleconnection* is a dynamical linkage between weather or climate variations occurring in widely separated regions of the globe (Murphree 2010d). Teleconnections resulting from the major climate variations, such as El Niño–La Niña (ENLN), the North Atlantic Oscillation (NAO), and the Indian Ocean Zonal Mode (IOZM) can be very significant (see Chapter II, Section A.2–A.4). While numerous studies have focused on the impact of these major climate variations to the Americas, east Asia, and the Pacific, relatively little research has been done to assess the impacts of these variations on SWA.

Vorhees (2006) assessed how these major climate variations influenced the fall-winter climate and weather in SWA. He found that anomalous convection in the maritime continent (MC) generates an anomalous tropical Rossby-Kelvin wave response (Matsuno 1966; Gill 1980) that often extends westward into the

northwest Indian Ocean (IO), affecting circulation patterns and moisture advection into SWA (Barlow et al. 2005, Vorhees 2006). ENLN and IOZM are often responsible for persistent fluctuations in MC convection and the resulting Rossby-Kelvin patterns (Vorhees 2006, LaJoie 2006). Climate variations in the Atlantic Ocean lead to the NAO, which also can affect conditions in SWA (Mariotti 2002, Cullen 2002, Vorhees 2006). See Vorhees (2006) for more information on the impact of these climate variations to SWA. Table 1 presents a summary of Vorhees' findings.

Table 1. Fall and winter precipitation anomalies in SWA due to climate variations (from Vorhees 2006). The pluses and minuses indicate a positive or negative phase of the climate variation, respectively.

	Fall	Winter
EN	Wet	Dry
LN	Dry	Dry / Wet
IOZM +	Wet	Dry
IOZM -	Inconclusive	Inconclusive
NAO +	~ Wet	Dry
NAO -	~ Dry	Wet

The Vorhees (2006) findings: (a) are not specific to Pakistan; and (b) are for the fall and winter seasons only. There have been very few studies of the impacts of climate variations on Pakistan in the peak precipitation months of Jul-Aug. Such studies have been conducted for neighboring regions in SWA and south central Asia (e.g., India). However, Pakistan is located on the boundary between the more arid regions of SWA to the west and the wetter south central Asian region to the east during the summer. The relative lack of prior studies of Pakistan climate variations during the summer was one of our motivations for conducting this study.

D. OPERATIONAL CLIMATE PRODUCTS FOR PAKISTAN

1. DoD Products

The Air Force Weather Agency (AFWA) is the chief Field Operating Agency (FOA) for Air Force Weather (AFW). AFWA's mission is to maximize America's power through the exploitation of timely, accurate, and relevant weather information. It oversees production of a suite of analysis and forecast products intended for use by warfighters (AFWA 2010b). AFWA is organized into two groups—the 1 Weather Group (WXG) and the 2 WXG. The 1 WXG is subdivided into operational weather squadrons (OWS) which offer weather support for specified regions of the world, while the 2 WXG provides specialized terrestrial, space and climatological global environmental intelligence information to both military and nonmilitary organizations. The 28 OWS (part of 1 WXG) and the 14 WS (part of 2 WXG) are the primary sources of DoD operational weather and climate products for Pakistan.

a. 28 Operational Weather Squadron

The 28 OWS, located at Shaw AFB, SC, provides weather information directly to Army, Navy, Marine, Air Force, and Coalition warfighters in the United States Central Command (CENTCOM) area of responsibility (AOR), which includes Pakistan (AFWA 2010b). While its primary responsibility to CENTCOM is to issue short-term forecasts and watches, warnings, and advisories (WWA), it has available to its forecasters a limited library of climatological data in the form of forecast reference notebooks (FRN). These FRNs and other analysis and forecast products are available at <https://weather.shaw.af.mil/>. Users need a password or a U.S. government common access card to view the suite of products at this site.

b. 14 Weather Squadron

The 14 WS, formerly known as the Air Force Combat Climatology Center, is located in Asheville, NC, and is the primary operational climate support

center for the U.S. Air Force and much of the rest of the DoD. Its mission is to rapidly disseminate climatological data to maximize combat effectiveness of DoD personnel and weapon systems (14 WS 2010). Customers include all branches of the military, and many civilian organizations within the DoD.

The 14 WS has recently started producing narrative-only LRFs (lead times of one to six months) of Pakistan surface air temperature, precipitation, and cloud ceilings. They include discussions of the state of ENLN as well as the expected departure from normal conditions. These LRFs are an attempt to improve on the traditional climatological products based only on LTM conditions that were until recently all that were available from the DoD (see Chapter I, Section E.4). Our study is an effort to improve the capability of DoD and others to produce skillful LRFs for Pakistan.

Long-range forecasts, narratives, and other products and services from the 14 WS are available at <https://notus2.afccc.af.mil/scis/>. Users need a U.S. government common access card to view the suite of products.

2. Non-DoD Products

a. *U.S. Products*

One of the missions of the National Oceanographic and Atmospheric Administration (NOAA) is “to understand and predict changes in climate” (NOAA 2011). NOAA provides the large majority of U.S. operational climate products currently available. The following list of U.S. based organizations that provide operational climate products includes three of NOAA’s subagencies directly responsible for creating such products.

(1) Climate Prediction Center (CPC). The CPC is the United States’ main provider of operational products for the prediction and monitoring of climate variability. Headquartered in Camp Springs, MD, its mission is “to deliver climate prediction, monitoring, and assessment products for timescales from weeks to years to the Nation and the global community for the protection of life and property and the enhancement of the economy” (CPC

2011). CPC provides a wide variety of climate assessments, outlooks, analyses, and forecasts for lead times of one week up to three months. Their suite of products is readily available at <http://www.cpc.ncep.noaa.gov/>.

(2) National Climatic Data Center (NCDC). The NCDC located in Asheville, NC, “is the world's largest active archive of weather data. NCDC produces numerous climate publications and responds to data requests from all over the world” (NCDC 2011). They operate the World Data Center (WDC) for Meteorology, which is one component of a global network that facilitates international exchange of meteorological data. The NCDC “acquires, catalogues, and archives data and makes them available to requesters in the international scientific community” (NCDC 2011). Much of this data is available online at <http://www.ncdc.noaa.gov/oa/ncdc.html>.

(3) Earth System Research Laboratory (ESRL), Physical Sciences Division. The focus of the ESRL Physical Sciences Division, located in Boulder, CO, is “to conduct weather and climate research to observe & understand Earth's physical environment, and to improve weather and climate predictions on global-to-local scales” (ESRL 2010). ESRL's interactive plotting and analysis tools give users access to a very useful datasets, the National Centers for Environmental Prediction (NCEP) / National Center for Atmospheric Research (NCAR) reanalysis dataset. These plotting tools are available at <http://www.esrl.noaa.gov/psd/>. We extensively used the ESRL tools and the NCEP/NCAR reanalysis dataset in this study, as discussed in Chapter II, Section A.

(4) International Research Institute for Climate and Society (IRI). IRI is a component of Columbia University located in Palisades, NY. IRI's mission is to increase society's awareness of the impact of climate on developing countries, and to provide scientific support for anticipating and managing these impacts more effectively (IRI 2011). The IRI produces seasonal climate forecasts including products for SWA and south central Asia (<http://portal.iri.columbia.edu/portal/server.pt>).

b. Non-U.S. Products

(1) European Centre for Medium-range Weather Forecasts (ECMWF). ECMWF is an international organization based in Reading, UK, that provides medium-range weather forecast support to European meteorological organizations. The ECMWF develops numerical methods for medium-range weather forecasting and distributes medium-range forecasts to its customers. ECMWF also runs a seasonal forecasting system that produces forecasts out to six months (<http://www.ecmwf.int/>).

(2) United Kingdom Meteorological Office (UKMO). The UKMO is the UK's National Weather Service and supports UK defense forces. They have a subsidiary climate service branch which focuses on the research and science of climate change (<http://www.metoffice.gov.uk/>).

E. MOTIVATION AND SCOPE OF THIS STUDY

1. Geopolitics and National Security

In Chapter I, Section A, we introduced the threats posed to U.S. national security by climate-related natural disasters in Pakistan. The nation of Pakistan, in a broad sense, is a key ally of the United States, as both countries have taken a similar stance in combating terrorism (Ahmad 2010). The two governments maintain an open dialogue with one another regarding security within the region. Despite this generally civil dialogue, many challenges remain. United States and Pakistani counterterrorism policies have converged in some areas, yet noticeable incompatibilities remain in others, as Pakistan has yet to undertake the shift in its regional counterterrorism approach that the U.S. demands (Ahmad 2010). For example, a disconnect still exists between Pakistan's "approach of practicing toughness toward home-grown domestic terrorists and leniency toward home-based regional terrorists" (Ahmad 2010). While the United States would like to have a long-term strategic relationship with Pakistan, there is a significant risk

that an unforeseen destabilizing event could create conditions that allow extremists groups to exert more influence within Pakistan's government structure (Ahmad 2010).

The 2010 floods brought to the forefront the reality that climate and weather play a critical role in the stability of Pakistan. In early July 2010, before the floods occurred, U.S. Secretary of State Hillary Rodham Clinton announced more than \$500 million in assistance projects for Pakistan, including funds for improving health and medical facilities, water management and distribution, farm productivity and agricultural marketing opportunities, and energy (Kaufman 2010). The Jul-Aug 2010 floods wiped away many of those projects. The United States was quick to pledge another \$390 million in immediate relief and recovery efforts for Pakistan, as well as technical and military assistance, in what officials said was the largest humanitarian crisis the international community had ever confronted (Kaufman 2010). The Office of the U.S. Special Representative for Afghanistan and Pakistan specifically cited the "strategic nature of the relationship with Pakistan" as the reason for the overwhelming response by the U.S. (Kaufman 2010).

The United States has made clear its intent to maintain the integrity of this strategic relationship. The summer of 2010 drew attention to the threat that climate variations pose in destabilizing Pakistan and undermining this relationship, thus impinging on the national security interests of the United States. The ability to forecast the conditions that lead to these extreme weather events at long lead times could mitigate the impact by allowing U.S. civilian leadership adequate time to converse with Pakistan about the potential risks and allowing both countries to prepare accordingly.

2. Military Operations

The DoD's 2010 QDR (see Chapter I, Section A) stated that "climate change will shape the operating environment, roles, and missions that we undertake" (U.S. DoD 2010). The 2010 floods in Pakistan provide evidence of

the truth of this statement. While the primary mission of U.S. military forces in SWA is to support both war efforts and peacekeeping within the region, in this case the U.S. military took on the role of humanitarian assistance and disaster relief (HA/DR). During the height of the crisis, 26 U.S. helicopters rescued more than 23,000 people and delivered more than 16 million pounds of refugee supplies (Kaufman 2010). U.S Air Force (USAF) Special Operations Weather Team (SOWT) member Captain Jonathan Sawtelle submitted an essay to us that further confirmed the ever-increasing role of HA/DR, and the types of missions required:

It is imperative from a regional security standpoint to assist populations whose governments are requesting HA/DR. HA/DR operations require air mobility: global reach to rapidly transport equipment, manpower and supplies to the region, and intra-theater airlift, which includes airdrops, helicopters, short take-off and landing (STOL) aircraft. Vehicles and ATVs have a limited reach but can be essential to localized distribution. (J. Sawtelle, personal communication)

Sawtelle also commented on the complexity and urgency of HA/DR plans, and stressed how dependent they are on long-range and short-range forecasts to best synchronize efforts and ensure safety of friendly forces.

The U.S. Navy also recognizes the rising interest in HA/DR and related contingencies. It recently conducted a gaming exercise at the Naval War College in Newport, RI, to practice scenarios in which the Navy might have to support U.S. or international relief efforts to help maintain regional and global stability. In each scenario, a climate-induced disaster triggered a catastrophic death toll, migration, and panic affecting regional or global security. The UN then issued a humanitarian response resolution. The training effort was the first of its kind to address this level of strategic military planning for a climate-induced disaster. It brought together a unique collaboration of climate scientists, water experts, health practitioners, logisticians, diplomats, aid workers, and military officers to think through options and responses (Baker 2010).

Of course, military missions in Pakistan are not only limited to HA/DR. Pakistan is also a major supply route for the war effort in Afghanistan (Baker 2010). Air Force Special Operations Command (AFSOC) frequently calls on the SOWT to perform environmental reconnaissance, in addition their routine work of collecting and communicating weather observations. The SOWT also deploys to survey rivers with handheld kits and fly small unmanned aerial vehicles so they can report critical information on rapidly changing environmental conditions.

Regardless of the mission, the U.S. military is becoming increasingly aware of the impact of climate to its forces in the field. “Therefore forecasting long-range changes in weather (2–4 months), climate, and having the capability to articulate these effects to the right planners can ensure safe and timely mission execution and enable an advantaged planning cycle over enemy forces” (Sawtelle 2010).

3. Air Force Weather Operations

More specifically, the Air Force Weather (AFW) career field needs accurate LRFs to be able to perform its mission more effectively. One of the topics currently among the highest priorities according to AFW is long-range forecast improvement with a focus on the SWA region (AFWA, personal communication). The research conducted in this study directly addresses this topic. We anticipate that the methods and results of this study will ultimately improve the day-to-day operations of AFW.

4. Advanced Climate Analysis and Long-Range Forecasting in DoD

Rear Admiral David Titley, Oceanographer of the Navy, and Dr. Tom Murphree of the Naval Postgraduate School (NPS) have advocated for improved climate analysis and long-range forecasting by DoD to improve the planning and outcomes of DoD operations. In simple terms, they have supported the application of state-of-the-science climate data sets and methods to support DoD operations (Murphree 2010a). This concept is also known as smart climatology,

warfighter climatology, and climate science and operational support. The main idea is to use data sets and models with high spatial and temporal resolution, plus advanced statistical and dynamical forecasting methods, to provide more complete analyses and long-range forecasts of Earth's climate system than are presently being provided by DoD. Advanced climate analysis and long-range forecasting have the potential to substantially improve long-range support for warfighters (Murphree 2010a). Figure 7 provides a simple example of how traditional climatology and smart climatology differ from each other.

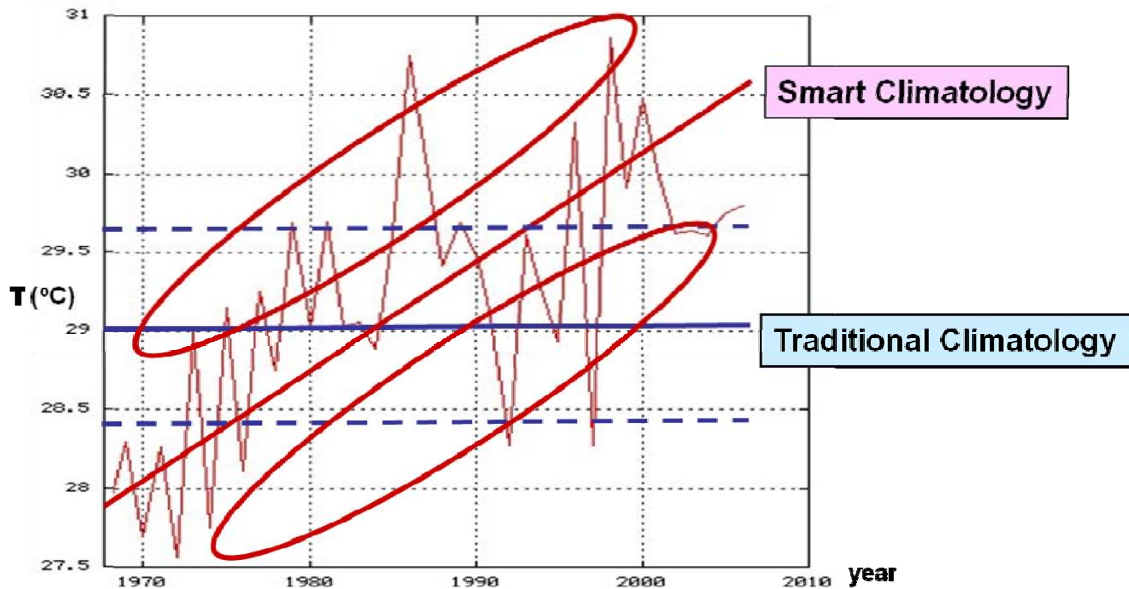


Figure 7. Time series of Jul–Sep surface temperature ($^{\circ}\text{C}$) in Iraq from 1968–2005. The solid and dashed blue lines represent the long-term mean surface temperature and long-term mean range, which are the basis for the traditional climatology approaches typically used by DoD in providing climate support. The solid red line and red ovals highlight the interannual and long-term trend in the surface temperature, which are examples of the additional types of climate information that are exploited when using smart climatology approaches to provide climate support. (From Murphree 2010a)

A number of prior studies conducted at the Naval Postgraduate School (NPS) have investigated the use of advanced climate analysis and long-range forecasting approaches to improving DoD climate support. Several of these

studies have extensively tested and developed methods to create long-range forecast systems for regions deemed a high priority by the DoD. These prioritized regions include SWA, Africa, and North America (e.g., Vorhees 2006, LaJoie 2006, Stepanek 2006, Moss 2007, Hanson 2007, Montgomery 2007, Tournay 2008, Lemke 2010), as well as oceanic regions around the globe (e.g., Turek 2007, Twigg 2008, Mundhenk 2009, Ramsaur 2009, Heidt 2009, Stone 2010).

5. Research Questions

This study explored the viability of using advanced climate datasets and methods to skillfully forecast atmospheric conditions at intraseasonal to seasonal lead times (e.g., leads of 0-6 months) to improve the planning processes of both DoD and non-DoD organizations. We focused primarily on investigating the following questions:

- (1) What atmospheric variables in Pakistan are both operationally significant and predictable at long lead times?
- (2) What climate system variables are the most viable predictors of climate variations in Pakistan, and can these variables be used to skillfully predict atmospheric conditions in Pakistan at long lead times?
- (3) What are the best LRF methods to use at all lead times in Pakistan?
- (4) What are the best formats for presenting LRFs to planners preparing for operations in Pakistan?

Chapter II provides an overview of the datasets and the methodology for climate analysis and LRF testing that we used in this study. Chapter III presents the results of our climate analysis and long-range hindcasts, and proposes potential LRF models. Chapter IV contains a summary of our results, conclusions, and recommendations for future research.

II. DATA AND METHODS

A. DATASETS AND SOURCES

1. NCEP/NCAR Atmospheric Reanalysis

The primary dataset we used in this study was the NCEP/NCAR reanalysis (R1) dataset (Kalnay et al. 1996; Kistler et al. 2001). This dataset is the result of a global retrospective analysis (i.e., a reanalysis) of atmospheric and sea surface conditions from January 1948 to present. The reanalysis is based on global observations collected via satellite, rawinsonde, aircraft, and land and sea-based in situ sensors. The dataset has a standard temporal resolution of six hours and a spatial resolution of 2.5° at standard tropospheric and stratospheric levels (Kalnay et al. 1996).

The NCEP/NCAR R1 dataset is particularly useful due to its uniform global coverage, accessibility, and ability to capture climate variations. Additionally, NOAA's ESRL website provides analysis and plotting tools to produce graphical representations of the data (see Chapter I, Section D.2.a.3). We used the R1 dataset and the ESRL website to generate many of the analysis figures for this study. NCEP has recently released a new coupled atmosphere-ocean-land-ice reanalysis dataset called the Climate Forecast System Reanalysis (CFSR). See Chapter IV, Section B for a discussion of the CFSR.

Even though the R1 dataset dates back to 1948, we chose to focus our study from 1970–2010 only. The reason for this was to maximize the impacts of satellite era data by eliminating data prior to 1970, while also working with a period long enough to represent interannual and decadal climate variations. Our main atmospheric variables of interest were sea surface temperature (SST, $^{\circ}\text{C}$), surface air temperature ($^{\circ}\text{C}$), GPH (m) at multiple levels, 850 hPa vector winds (m/s), and PR (mm/day).

2. Multivariate ENSO Index (MEI)

The MEI is a comprehensive representation of the ENLN phenomenon based on the six main observed variables over the tropical Pacific (MEI 2010). These six variables are: (1) sea-level pressure, (2) zonal surface wind, (3) meridional surface wind, (4) sea surface temperature, (5) surface air temperature, and (6) total cloudiness fraction of the sky (MEI 2010). Since the index is comprised of multiple variables, it is considered a more stable and integrated representation of ENLN than other indices that monitor only a single variable (e.g., Nino3.4 SST). Negative (positive) values of the MEI represent LN (EN), also known as the cold (warm) ENLN phase. For the purposes of our study, we analyzed the MEI as a possible predictor of Pakistan PR.

3. North Atlantic Oscillation (NAO)

A number of different methods have been developed to quantify the positive and negative phases of the NAO. The traditional definition for the NAO is the normalized pressure at a station in the Azores minus that of a station in Iceland. The intent is to measure the oscillation of mass between the Azores High and the Icelandic Low. An extended version of the index can be derived for the winter half of the year by using a station in the southwestern part of the Iberian Peninsula (Hurrell 2006). NOAA's ESRL uses the former method to construct an NAO index (NAOI), and we tested that index as a potential predictor of Pakistan PR for our study.

4. Indian Ocean Dipole Mode Index (DMI)

Another variable we analyzed as a possible predictor for Pakistan PR was the IO Dipole Mode Index (DMI), also known as the Indian Ocean Zonal Mode (IOZM). The DMI is based on the SST anomaly (SSTA) in an area of the eastern tropical IO minus the SSTA in an area of the western tropical IO (Saji et al. 1999). The area in the eastern tropical IO is at approximately 90°E–110°E and 10°S–0°N. The area in western tropical IO is at approximately 50°E–70°E and 10°S–10°N. A positive (negative) value in the DMI indicates a positive (negative)

phase in the Indian Ocean Dipole (Saji et al. 1999). We obtained values for the DMI from the Bureau of Meteorology (BOM 2010) in Australia and the Japanese Agency for Marine-Earth Science and Technology (JAMSTEC 2010).

B. CLIMATE ANALYSIS AND FORECASTING METHODS

The analysis and forecasting methods as investigated in this study are similar to those used by Heidt (2009) in her study of LRFs of ocean conditions in the western North Pacific, and Lemke (2010) in his study of LRFs of PR in the HOA.

1. Predictand Selection

The predictand, or forecast target, for our study was area-averaged precipitation rate (PR) for a selected region within Pakistan in July-August (Jul-Aug). Refer to Chapter I, Section E to see the rationale for choosing that predictand, and see Chapter I, Section B.2.a for why we chose that particular period.

The rationale for choosing an area-averaged predictand was that it is simply a larger forecast target than a specific point, meaning that it tends to be less susceptible to spatial and temporal variations. Area-averaged predictands also tend to: (a) make the development of the forecast method simpler; (b) increase predictability at long lead times; and (c) simplify forecast verification (van den Dool 2007). However, an area-average predictand may average out important spatial and temporal variability within the region of interest, if the area is not well chosen.

While choosing our predictand variable was straightforward, the process of choosing our predictand region within Pakistan was rather lengthy. We analyzed long-term mean and interannual Jul-Aug PR anomalies within Pakistan to get an understanding of how precipitation is spatially distributed within the country. These results prompted us to consider several different predictand regions, and ultimately we chose a single region that best met our requirements

(described in Chapter III, Section A). The major features we considered in choosing the predictand region were:

- Spatial patterns in LTM PR in and near the region
- Spatial patterns in the interannual and decadal scale PR anomalies in and near the region
- Anomalous PR in the most recent decade
- The impact of anomalous PR in the region and on the rest of the country (e.g., downstream flooding)
- Significant correlations between PR in the region and major climate variations (e.g., MEI, NAO, DMI) at lead times of zero to six months
- Significant correlations between PR within the region and potential atmospheric and oceanic predictors (e.g., global SST) at lead times of zero to six months

2. Composites, Correlations, and Teleconnections

After we established our predictand region, we created a time series of PR from Jul-Aug 1970–2010 within that region. We used this time series to determine the eight wettest (driest) years on record. We then used the ESRL mapping and analysis tools to create Jul-Aug seasonal composites of other environmental variables during the same eight wettest (driest) years. The purpose of this exercise was to identify the atmospheric patterns and processes that lead to above normal (AN), near normal (NN), and below normal (BN) PR anomalies in Pakistan. We examined both composite means and anomalies of regional PR (mm/day), global SST ($^{\circ}$ C), GPH (m), 850 hPa vector winds (m/s), outgoing longwave radiation (OLR; W/m²), 850 hPa specific humidity (g/kg), and 700 hPa omega (Pa/s). We calculated all anomalies in this study using a base period of 1968–1996 (cf. ESRL 2010).

Once we had an understanding of the basic atmospheric processes, we identified potential long lead predictors for the predictands. We correlated the time series of Pakistan PR with other environmental variables (e.g., winds, SST, temperature, GPH) on a global scale, with the potential predictors leading the

Jul-Aug predictand by zero to six months at bi-monthly intervals. We found teleconnections by identifying significant correlations between the predictand and remote potential predictors. Based on the full study period of 1970–2010, we considered correlations greater than $+/-.30$ statistically significant at a 95% confidence level based on the standard normal distribution of a two tailed t test (Wilks 2006). When we reduced the dataset to 11 years for our optimal climate normal analyses (2000–2010), we considered correlations greater than $+/-.55$ to be statistically significant at a 95% confidence level. We performed the correlation analyses using Microsoft Excel and the ESRL website (ESRL 2010).

3. Predictor Selection

We defined a potential predictor as a variable with significant long lead correlations, as well as dynamically plausible teleconnections, with the predictand. We investigated the plausibility of several potential predictor variables, with particular focus on SST and GPH.

We eventually chose 850 hPa GPH as our main predictor because: (a) it had the strongest correlations of any predictor analyzed; and (b) it had a clear, dynamically plausible relationship to the predictand. Yet while the predictor/predictand relationship was straightforward, 850 hPa GPH predictors at multiple locations were needed to capture the entirety of the relationship. Our final predictor for Pakistan PR was an index that combined the 850 hPa GPH anomalies of several regions in the general south central Asia region.

4. Predictor and Predictand Time Series

Once the main PR predictand and corresponding predictors were chosen, we analyzed their time series to identify intraseasonal to decadal patterns of variability in the predictors and predictands, and in their correlations with each other. We also used the time series to identify extreme events for use in conditional composite analyses and multi-year trends that might influence the selection of long-range forecasting methods.

After we chose the predictors, we compared the predictor and predictand time series to identify the correspondence of interannual variability as well as the significance of the overall correlation. This process also allowed us to: (a) perform a visual quality control check of the predictor-predictand relationship; (b) identify periods and lead times for which the correlations were relatively strong and weak; and (d) identify case studies for additional composite, correlation, and dynamical analyses, and hindcast testing.

5. Long-Range Forecast Method Development and Hindcast Testing

We developed and assessed several LRF methods for this study in order to improve upon: (a) the LTM forecast methods commonly used by DoD forecasters, and (b) the LRF methods presently being used by 14 WS and other non-DoD organizations. Prior studies have shown that forecasts that take into account deviations from the LTM (i.e., anomalies) have greater potential for accuracy than those based on the LTM alone (cf. Chapter I, Section E.4). In addition, LRFs based on customized predictors selected for a specific forecast target often have more skill than those based on standardized climate variations, such as ENLN (e.g., Heidt 2009, Lemke 2010).

In order to assess the viability of a predictor, we employed the forecast methods to conduct hindcast testing of the predictor-predictand relationship for the 1970–2010 period. We then assessed the skill of the predictor using the thresholds we set for each individual method. We used Microsoft Excel to perform the tests and quantify the results for each of the hindcast testing methods conducted.

a. *Linear Regression*

A simple linear regression model describes the relationship between two variables. In our case, the two variables represent the predictor and the predictand (i.e., the independent variable and dependent variable, respectively; Wilks 2006).

As discussed in Chapter II, Section B.3, we formed our predictor by combining multiple predictors to create a single variable index. To determine which predictors to include in the index, we ran single variable linear regressions between each individual predictor, each combination of predictors, and our predictand (Pakistan PR), at zero lead. To measure the fit of each regression, we calculated the correlation coefficient, the coefficient of determination (R-square), adjusted R-square, and significance F. For this single variable regression, we compared the findings (particularly the correlation coefficient) to assess the viability of each predictor (cf. Chapter II, Section B.2 for statistical significance thresholds).

We then conducted multivariate linear regressions to assess the viability of each predictor when combined into a single predictor index. We calculated the same metrics as in the single variable regression, with the addition of p-values. We considered p-values ≤ 0.05 to be statistically significant at a 95% confidence level. We ran multiple instances of this multivariate regression method in order to eliminate predictors that exceeded this p-value threshold. Our goal was to select an optimal combination of predictors from which to build a multivariate linear regression model to use in forecasting our predictand at leads of one to six months. We then ranked each instance by its adjusted R-square value and compared the p-values. Adjusted R-square is a preferred metric in multivariate regression (when compared to correlation or R-square), since it imposes a penalty for each added predictor (e.g., R-square only increases if the additional variable improves the model more than would be expected by chance), and is utilized to prevent overfitting. We eliminated predictors with p-values > 0.05 from consideration. Refer to Wilks (2006) for further information on linear regression.

b. Tercile Matching

For the tercile matching method, we sequentially sorted the 41 years of predictand and predictor values, and then identified for each year the

tercile categorical state of the predictand and predictor values. These tercile states are above normal (AN), near normal (NN), and below normal (BN), with each tercile representing approximately one-third of the total years. We used the sign of the predictor-predictand correlation to determine the expected relationships between the predictor tercile categories and the predictand tercile categories. For example, we identified a positive correlation between our 850 hPa GPH-based predictor index and Pakistan PR from Jul-Aug 1970–2010. Thus, we used the occurrence of an AN predictor value in 2010 to produce a hindcast of AN Pakistan PR for the same year. Similarly, we used a BN (NN) predictor value in a given year to produce a hindcast of BN (NN) for that same year. We then verified those hindcasts by comparing them to the tercile categorical state of the observed Pakistan PR.

Perhaps the most beneficial feature of tercile matching is its conceptual and computational simplicity. The results of this simple hindcast and verification method allowed for quick visual and quantitative assessments of the viability of the predictor-predictand relationship.

c. Hindcast Verification Methods

We verified the hindcasts by comparing the predictor and predictand AN, NN and BN tercile assignments for each year during 1970–2010. This allowed us to identify the hindcast for each year as a hit, miss, false alarm, or correct rejection. We then sorted these hindcast verification results into a 2 x 2 contingency table (Table 2; Wilks 2006).

Table 2. Schematic contingency table used to verify hindcasts of Jul-Aug Pakistan PR. The cells of the table represent the number and combinations of observed occurrences (obs Y), observed non-occurrences (obs N), predicted occurrences (pred Y), and predicted non-occurrences (pred N) of Pakistan PR. A separate contingency table was used for each of the three tercile categories for Pakistan PR (AN, NN, and BN). We used the values from this table to calculate several hindcast verification metrics including accuracy rate, probability of detection (POD), false alarm rate (FAR), and Heidke skill score (HSS). (After Wilks 2006)

	obs Y	obs N	
pred Y	a	b	a + b
pred N	c	d	c + d
	a + c	b + d	Yrs Total

We performed a separate contingency table test for each of the AN, NN, and BN categories. The following is an explanation of the values that we input into the table for the AN category:

a = AN was hindcasted and observed

b = AN was hindcasted and BN (NN) was observed

c = BN (NN) was hindcasted but AN was observed

d = BN (NN) was hindcasted and BN (NN) was observed

Total number of forecasts = $n = a + b + c + d$ = total number of years = 41

From our contingency table results, we calculated four different verification metrics: accuracy rate or percent correct, false alarm rate (FAR), probability of detection (POD), and Heidke skill score (HSS). See Wilks (2006) for a definition of each metric. The following equations show how each metric was calculated (Wilks 2006):

1. $Accuracy = (a + d) / n$
2. $FAR = b / (b + d)$

$$3. \text{ } POD = a / (a + c)$$

$$4. \text{ } HSS = 2[(ad) - (bc)] / \{[(a + c)(c + d)] + [(a + b)(b + d)]\}$$

Larger (smaller) values of accuracy rate, POD, and HSS indicate higher (lower) skill. Smaller (larger) values for FAR indicate higher (lower) skill. The HSS essentially attempts to eliminate the probability of a correct forecast attributed to randomness. It uses a scale of minus one to plus one, with the best HSS being equal to one. A HSS of less than zero (equal to zero) means that the hindcast is worse (no better) than using LTM climatology.

We used the following three criteria to determine the viability of each predictor-predictand pair. We considered hindcasts that met all three criteria to be skillful and viable:

1. Accuracy greater than 50%
2. POD equal to or greater than FAR
3. HSS values greater than 0.3

d. Optimal Climate Normals

Optimal climate normals (OCN) is an approach to long-range forecasting in which trends in the predictand over the most recent years are used to produce a LRF. This approach is based on the concept that in a slowly varying climate, recent trends may provide better estimates of the upcoming expected value than other LRF approaches (van den Dool 2007). The standard process of applying this method is to calculate a mean value for a selected range of consecutive recent years (e.g., most recent 10–15 years), then persist that mean forward in time to produce a forecast for the following year (van den Dool 2007).

We applied the OCN approach by regrouping our tercile categories (see Chapter II, Section B.4.b) based on the most recent 11 years of data (Jul-Aug 2000–2010), and reinvestigated the predictor-predictand relationship through the hindcast testing methods described throughout this section. These

results yielded new, well-correlated, dynamically plausible predictors for the 2000–2010 period. We tested these new predictors by using the same hindcast testing methods. The result was a separate and skillful predictor index for Pakistan PR based on predictand-predictor relations during 2000–2010.

While we did adhere to the general principles of the OCN concept in our study, we did not replicate the standard OCN process of using the mean of the recent trend (2000–2010) to produce a forecast. Instead, we simply applied the basic concept of emphasizing recent conditions when developing forecast methods, which led us to the development of a second predictor index for Pakistan PR based on just the last 11 years of data.

6. Forecast Systems Development

While the majority of our study focused on the hindcast testing discussed in the previous section, we did develop recommendations for developing a forecast system for Pakistan PR based on our results. Those recommended forecast systems are: (a) a direct statistical model; (b) a direct dynamical model; and (c) statistical-dynamical model. We also analyzed some preliminary data to assess the potential skill of each of these three models.

C. SUMMARY OF CLIMATE ANALYSIS AND FORECASTING METHODS

Figure 8 summarizes the analysis and long-range forecasting and hindcasting methods we used in this study. The reanalysis dataset allowed us to analyze the environmental patterns associated with anomalous values for our predictand, and to identify dynamically plausible predictor-predictand relationships. We then tested the relationships via hindcasts, to form the basis for developing a forecast system that will produce LRFs with greater skill than what is currently available.

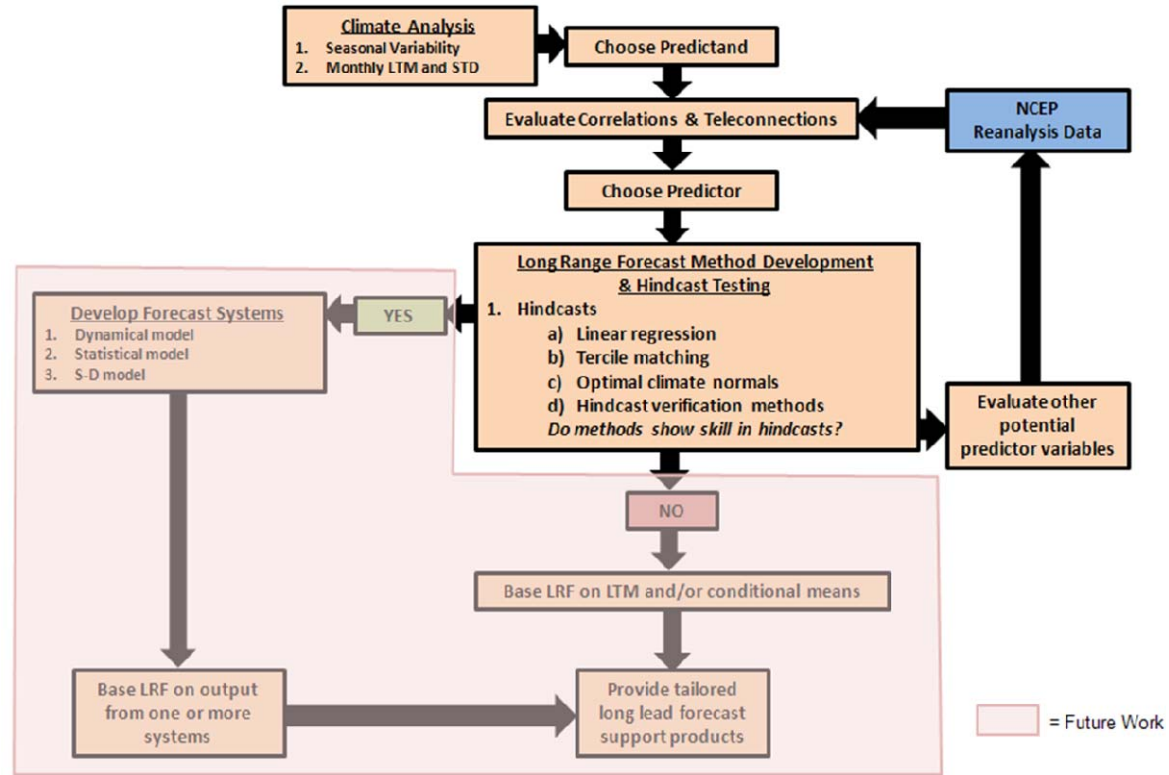


Figure 8. Flow chart showing main datasets and methods used to conduct climate analyses and long-range forecasts in this study and recommendations for future studies. (Adapted from Lemke 2010)

III. RESULTS

A. CLIMATE ANALYSIS RESULTS

1. Predictand Selection

We chose our predictand variable as Jul-Aug Pakistan PR (see Chapter I, Section B.2.a). However, as mentioned in Chapter II, Section B.1, the selection of our predictand region within Pakistan was a lengthy task. We analyzed interannual composite mean and anomalous PR during 1970–2010 and during 2000–2010, and discovered a range of PR and PR anomaly distribution patterns. We investigated three different predictand regions within Pakistan (Boxes 1-3 in Figure 9) and settled on one of these as our primary predictand region (Box 2 in Figure 9). We first investigated Box 1 because it enclosed a region with pronounced LTM PR patterns (Figure 10a) and PR anomalies during 1970–2010 (not shown). However, Box 1 included regions with large PR anomalies during 2000–2010 that differed in sign (Figure 10b). Based on these PR anomalies, we investigated using Box 2 and Box 3 as PR predictand regions.

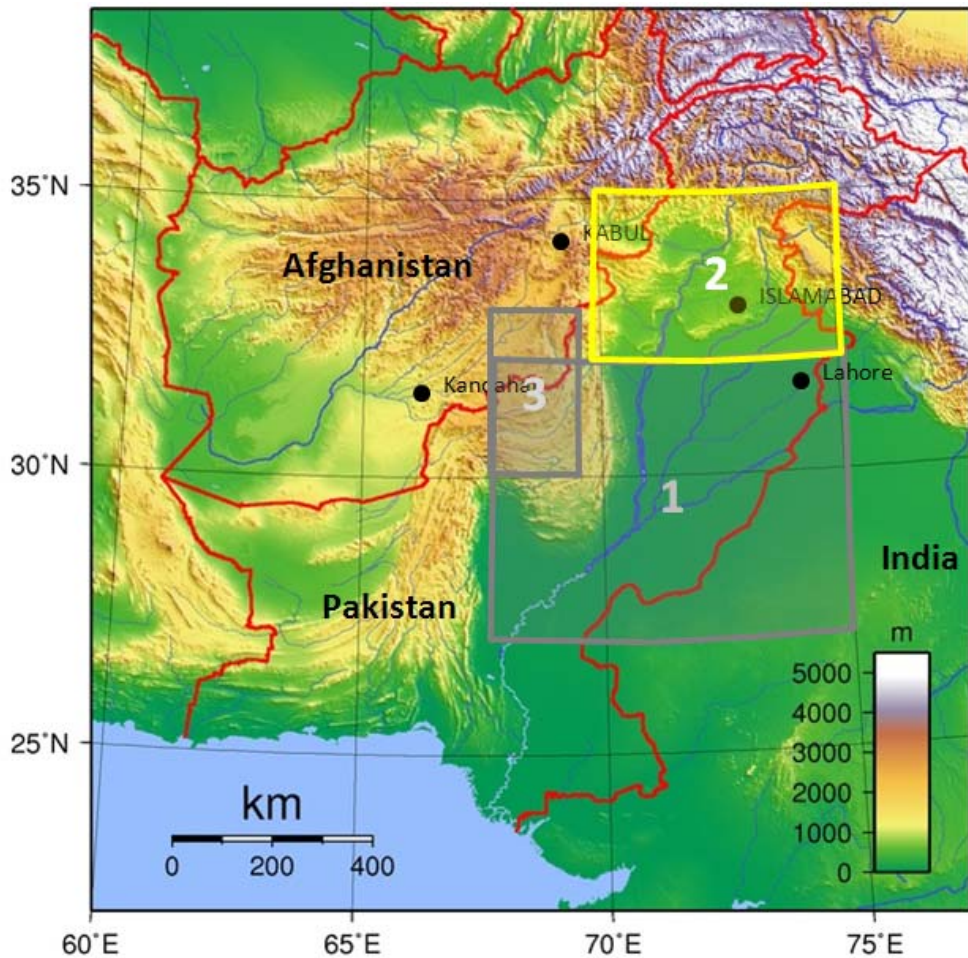


Figure 9. Physical relief map of Pakistan overlaid with the three predictand regions considered in this study. The coordinates for the predictand regions are: (a) Box 1: 27° – 32° N, 67° – 75° E; (b) Box 2: 32° – 35° N, 70° – 75° E; and (c) Box 3: 30° – 33° N, 67° – 69° E. After conducting the analysis methods described in Chapter II, Section B, we ultimately chose Box 2 (outlined in yellow) as our main predictand region. (“Pakistan Topography,” after Wikipedia 2010; available online at: http://upload.wikimedia.org/.../Pakistan_Topography.png)

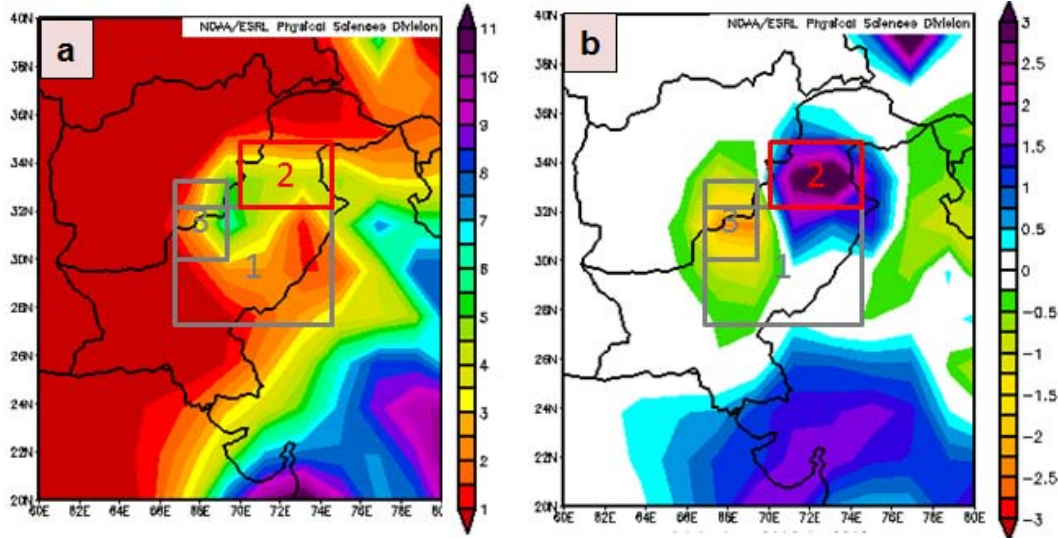


Figure 10. (a) Jul–Aug LTM PR (mm/day); and (b) Jul–Aug 2000–2010 PR anomaly (mm/day). The predictand boxes considered for this study are overlaid. We initially chose each box as a potential predictand after analyzing annual PR patterns from 1970–2010. Ultimately, we selected Box 2 after considering: (1) the LTM PR amounts and variations; (2) the 2000–2010 PR amounts and variations; and (3) the impact to flooding. Thus, all references to Pakistan PR throughout the remainder of this study refer to the Box 2 predictand region.

One of our criteria for selecting a PR predictand region was potential flooding impacts. The Box 2 region in north central Pakistan is where the heaviest rainfall fell in the Jul–Aug 2010 flooding event described in Chapter I. Note from Figure 9, that Box 2 lies at a higher elevation than most of the rest of Pakistan, and that an extensive river system flows through the region into the lower elevations. In 2010, heavy rain within the Box 2 region led to these rivers overflowing their banks downstream, which subsequently flooded much of the country.

We chose Box 2 as our main predictand because it met our criteria of: (a) relatively high LTM Jul–Aug PR (Figure 10a); (b) high potential impacts on downstream flooding and water supply (Figures 9, 10); and (c) distinct PR anomalies observed during recent years (2000–2010; Figure 10b). Additionally,

recall that the OCN approach places greater emphasis on the most recent trend, and Box 2 is an excellent representation of that trend. Consequently, all references to Pakistan PR throughout the remainder of this study shall refer to the PR predictand in the Box 2 region (Figures, 9, 10).

Figure 11 is a time series of that predictand, Pakistan PR, from 1970–2010. Clearly visible is an uptrend in PR since 1970, and especially since 2000, consistent with the anomaly in Figure 10b. Note that the mean PR for 2000–2010 is higher than the mean PR for 1970–1999. Also, note the spike in 2010 that resulted in major flooding event in Pakistan was the second highest Jul-Aug PR during the 41-year study period.

We used the PR time series in Figure 11 to identify the eight most extreme AN and BN PR events from 1970–2010. Based on this identification, we constructed composites of the atmospheric and oceanic conditions associated with extreme AN and BN Pakistan PR (see Chapter III, Section A.2). The purpose of these composites was to identify: (a) the major spatial and temporal patterns associated with, and the dynamical processes that lead to, climate variations in Pakistan PR; and (b) potential predictors of Pakistan PR variations (see Chapter II, Section B.2).

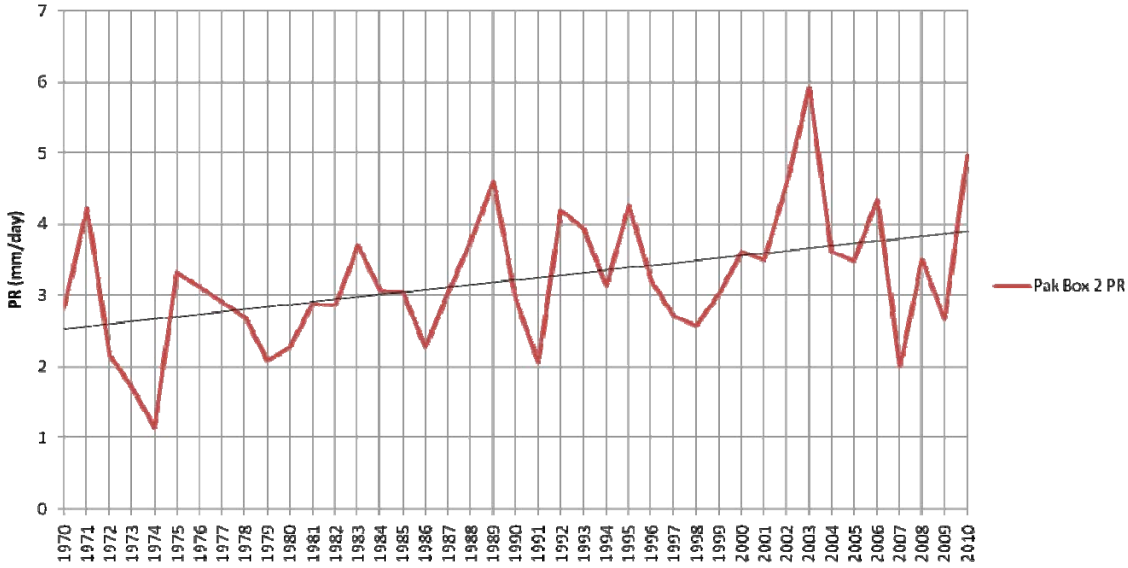


Figure 11. Time series of Jul–Aug Pakistan PR (mm/day) from 1970–2010. Note the uptrend of 0.35 mm/day per decade since 1970, and the spike in 2010 associated with the record flooding described in Chapter I, Section A.

2. Composite Analysis

a. Long-Term Means

We analyzed the prevailing, or long-term mean, environmental conditions in Pakistan and nearby regions during Jul–Aug. Understanding these climatological conditions is essential in determining the processes that produce Pakistan PR anomalies and in identifying potential predictors of Pakistan PR.

Figure 12a shows the LTM Jul–Aug PR for the SWA/south Asian region, while Figures 12b–12d show corresponding atmospheric conditions. Note the strong upper level ridge (Figure 12b) overlying a broad area of low heights in the lower levels of the troposphere (Figure 12d). The advection from the south of moist air into the lower tropospheric trough leads to high PR in south central Asia and arid conditions in the majority of SWA. Pakistan lies on the boundary between the arid region to its west and the wet region to its east, and has some of the characteristics of each region. The Somali jet, depicted in Figure 12c, flows northeastward along the coast of Somalia and into the Arabian

Sea. A northern branch of this jet supplies Pakistan with much of its moisture and precipitation during Jul-Aug. This summertime regime is known as the southwest monsoon (see Chapter I, Section B.2).

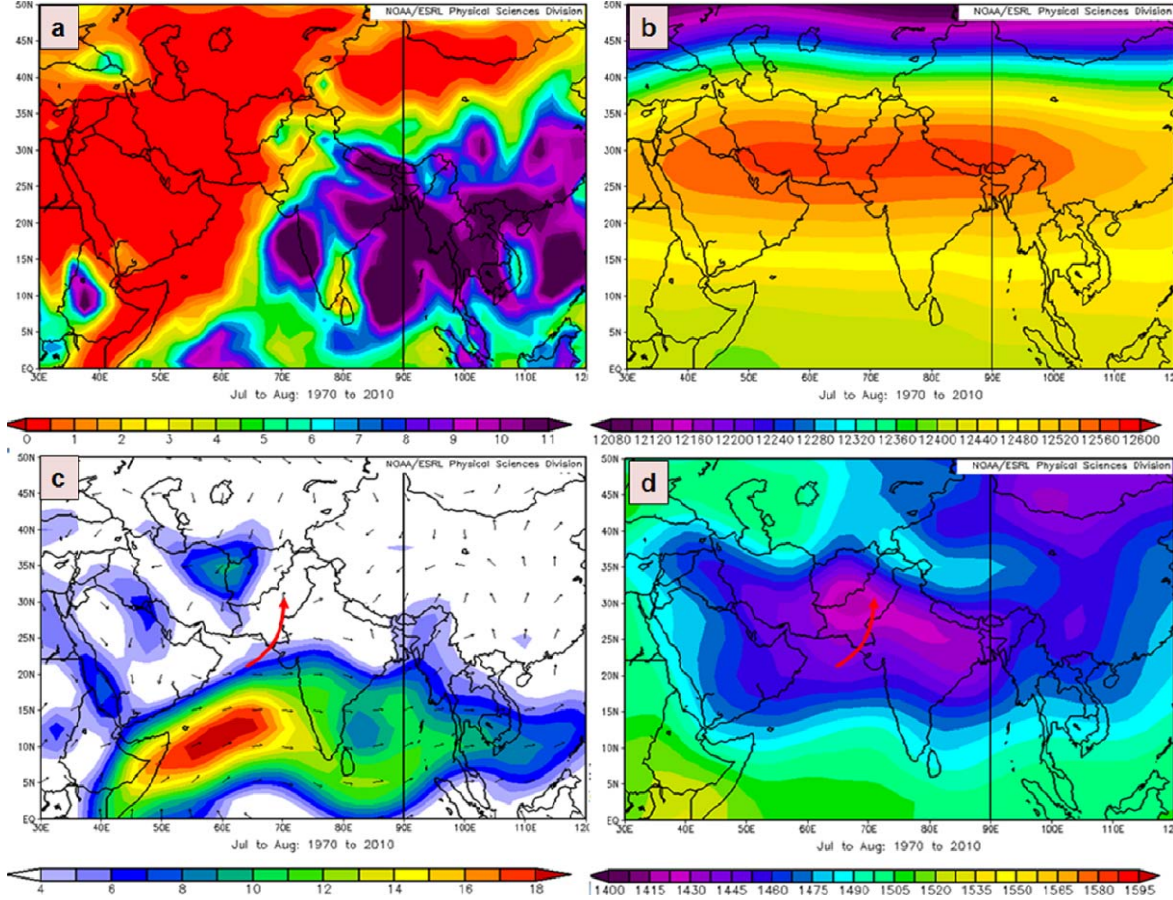


Figure 12. Jul–Aug LTM: (a) PR (mm/day); (b) 200 hPa GPH (m); (c) 850 hPa vector winds (m/s); and (d) 850 hPa GPH (m). Jul-Aug is characterized by a strong lower tropospheric trough over southern Asia (d) that is overlain by a strong upper tropospheric ridge (b). This height pattern allows for a northern branch of the Somali jet (red arrow in c, d) to bring moisture from the Arabian Sea into Pakistan (c, d) leading to high PR over much of southern Asia, with Pakistan lying just to the west of this high precipitation region.

Figure 13 also shows the LTM Jul-Aug PR (Figure 13a) along with additional atmospheric variables for the same time frame. Figures 13b and 13c are composites of outgoing longwave radiation (OLR) and 850 hPa specific humidity, respectively. Low values of OLR tend to indicate deep convection,

while higher specific humidity levels indicate the availability of moisture for precipitation. Pakistan is on the western (eastern) edge of the region in which conditions tend to be favorable (unfavorable) for precipitation. This suggests that Pakistan PR in Jul-Aug may be sensitive to small changes in the circulation and moisture of neighboring regions. For example, it suggests that above (below) normal PR periods in Pakistan may be associated with positive (negative) moisture advection anomalies into Pakistan from the south and east (north and west).

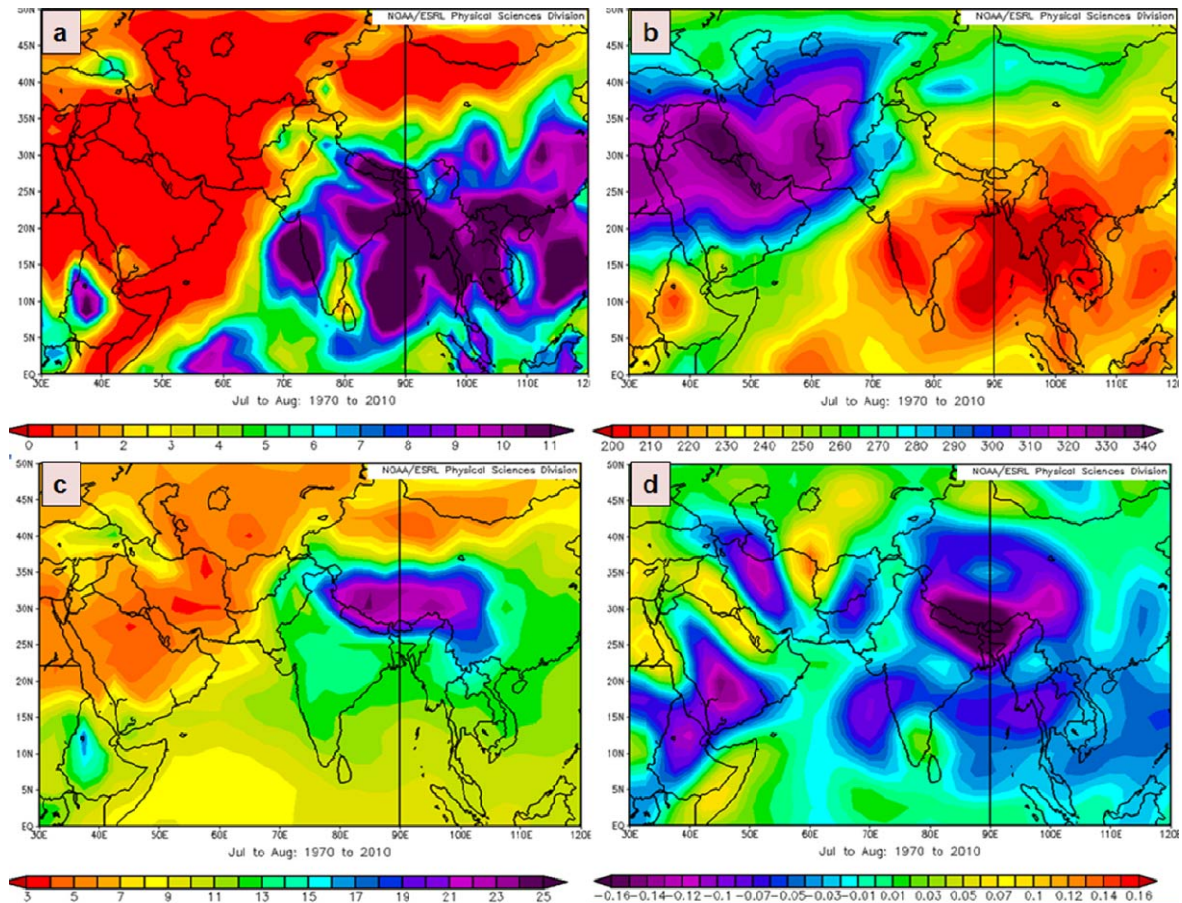


Figure 13. Jul–Aug LTM: (a) PR (mm/day); (b) OLR (W/m^2); (c) 850 hPa specific humidity (g/kg); and (d) 700 hPa omega (Pa/s). As expected, high PR (a) tends to be associated with low OLR (b), high 850 hPa specific humidity (c), and upward vertical motion (d). Pakistan lies on the western (eastern) edge of the region in which conditions are favorable (unfavorable) for high PR (cf. Figures 12–13).

b. Conditional Anomalies

Once we had an understanding of the normal atmospheric patterns and processes in and around Pakistan for Jul-Aug, we needed to select potential long lead predictors for Pakistan PR. We used the Pakistan PR time series described in Chapter III, Section A.2, to identify for Jul-Aug 1970–2010 the eight most extreme high PR years (1971, 1989, 1992, 1995, 2002, 2003, 2006, 2010) and the eight most extreme low PR years (1972, 1973, 1974, 1979, 1980, 1986, 1991, 2007). We then constructed conditional composites of the anomalies for these extreme events. We designated these as the *wet* and *dry* composites, respectively. These composite anomalies conditioned on the occurrence of extreme AN and BN PR in our predictand region assisted us in indentifying regional and global scale patterns and processes that are related to extreme PR events in our predictand region.

Figure 14 shows the regional wet and dry composite anomalies for PR. Note that AN (BN) is associated with: (a) AN (BN) PR in the neighboring region of western India; and (b) BN (AN) PR in the eastern Bay of Bengal. The largest PR anomalies within Pakistan in the wet and dry anomalies are mainly in the north-central part of the country, consistent with the low PR in the northernmost and southernmost parts of Pakistan (cf. Figures 10a, 12a). These areas with the largest Pakistan PR anomalies are located within or near the PR predictand region (red boxes in Figure 14). It is also interesting that dry conditions in southern India are observed during either wet or dry PR extremes in Pakistan.

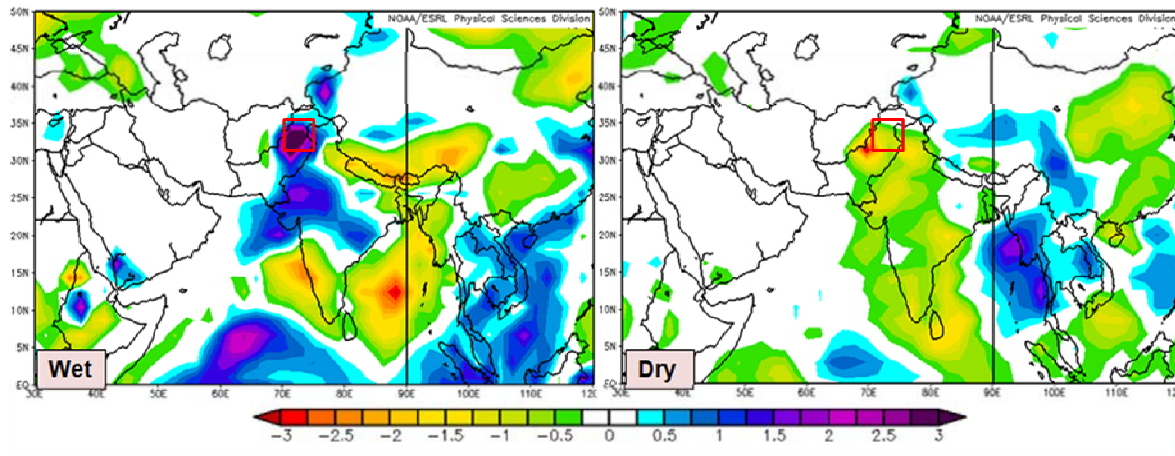


Figure 14. Conditional composite anomalies of PR (mm/day) for the eight most extreme wet (left panel) and dry (right panel) Pakistan PR events during Jul–Aug 1970–2010. The red boxes outline our predictand region. Note the isolation of the anomalies to the north-central portion of Pakistan, in and close to the predictand region.

Figure 15 shows the global wet and dry composite SST anomalies (SSTAs). Notice the overall lack of strong SSTA patterns in either the wet or the dry years, and the absence of clear indications of ENLN patterns in the SSTAs. This indicates that SST is most likely not a good direct predictor of Jul–Aug Pakistan PR, even though SST is a good predictor for many other climate variations (e.g., Vorhees 2006, Moss 2007, Lemke 2010).

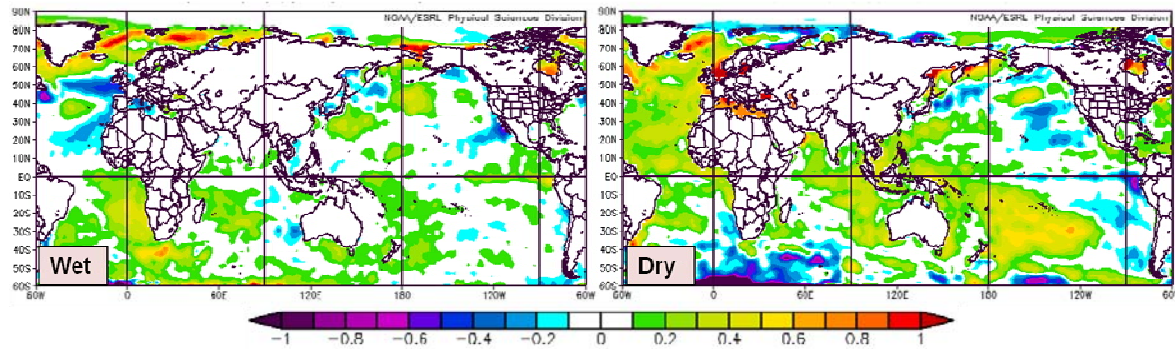


Figure 15. Conditional composite anomalies of SST ($^{\circ}$ C) for the eight most extreme wet (left panel) and dry (right panel) Pakistan PR events during Jul–Aug 1970–2010. Note the general absence of strong clear patterns in either wet or dry year composites. This indicates that SST may not be a good direct predictor of Pakistan PR.

Figure 16 displays the wet and dry composite anomalies for 850 hPa GPH. The red arrows denote the direction of the corresponding implied anomalous flow. In the wet composite, AN 850 hPa GPH are observed over Nepal, with less clear BN GPH over the Red Sea. The resulting low-level flow is southerly and convergent over and near Pakistan, with an implied positive moisture advection from the tropical IO and Pacific, and from the Arabian Sea. Conversely, the dry composite shows BN 850 hPa GPH over Nepal coupled with AN GPH in the Caspian Sea region. These anomalies lead to dry, offshore, divergent low-level flow over and near Pakistan.

These results are analogous to those from Vorhees (2006) in indicating that low-level positive (negative) moisture advection anomalies from the south and east (north and west) contribute to anomalously wet (dry) periods in SWA, although Vorhees focused on the fall and winter seasons only.

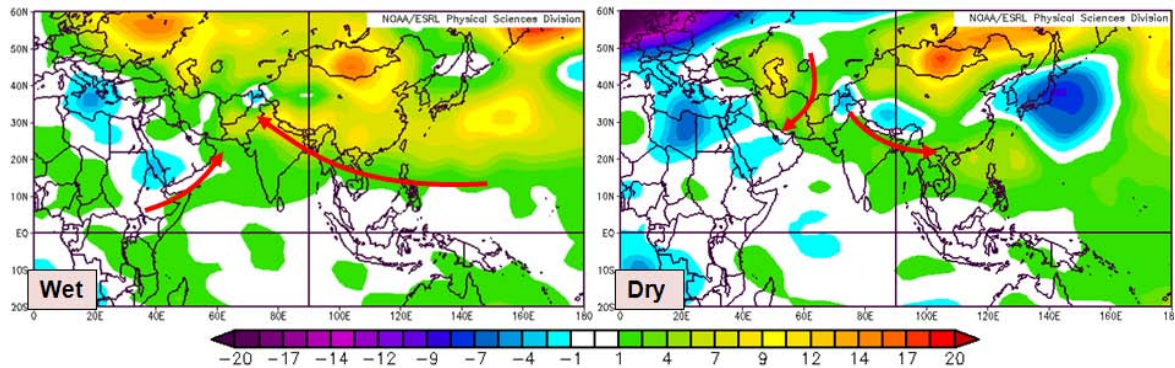


Figure 16. Conditional composite anomalies of 850 hPa GPH (m) for the eight most extreme wet (left panel) and dry (right panel) Pakistan PR events during Jul–Aug 1970–2010. The red arrows schematically represent the corresponding wind anomalies that are likely to affect Pakistan. Note in the wet (dry) composite the anomalous high (low) over the Nepal region providing a moist easterly (dry westerly) flow into Pakistan. Low-level convergent (divergent) flow also characterizes wet (dry) years over and near Pakistan.

Figure 17 shows the wet and dry composite anomalies for 700 hPa omega. Negative (positive) values of omega indicate upward (downward) vertical motion. Note that wet (dry) years are associated with a negative

(positive) omega anomaly over our PR predictand region (red box in Figure 17), as expected. This increase (decrease) in upward vertical motion is consistent with the low-level convergence (divergence) implied by Figure 16.

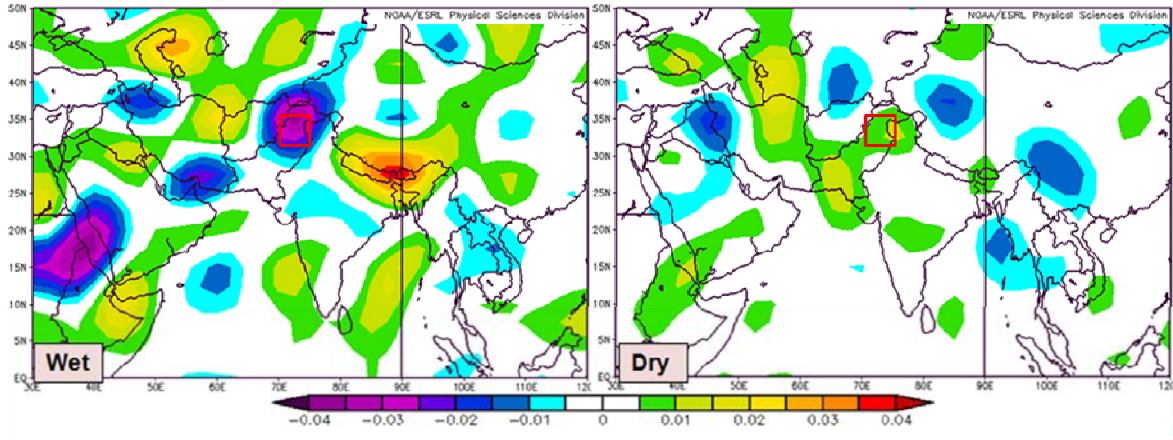


Figure 17. Conditional composite anomalies of 700 hPa omega (Pa/s) for the eight most extreme wet (left panel) and dry (right panel) Pakistan PR events during Jul–Aug 1970–2010. The red boxes outline our predictand region. Note in the wet (dry) composite the negative (positive) anomalies over Pakistan indicating an increase (decrease) in upward vertical motion.

Figure 18 shows the wet and dry composite anomalies for 850 hPa specific humidity. As expected, wet (dry) years are associated with higher (lower) specific humidity levels than normal. Note that the BN anomaly for the dry years encompasses both Pakistan and Afghanistan, while the AN anomaly during the wet years is more confined to Pakistan. We expect this is largely due to the topography of the region. While broad offshore, divergent flow characterizes dry years, in the wet years the mountains along the Afghanistan border may restrict westward moisture transport by the southerly to southeasterly low-level wind anomalies implied by the height anomalies in Figure 16. See Figure 9 to examine these topographical features.

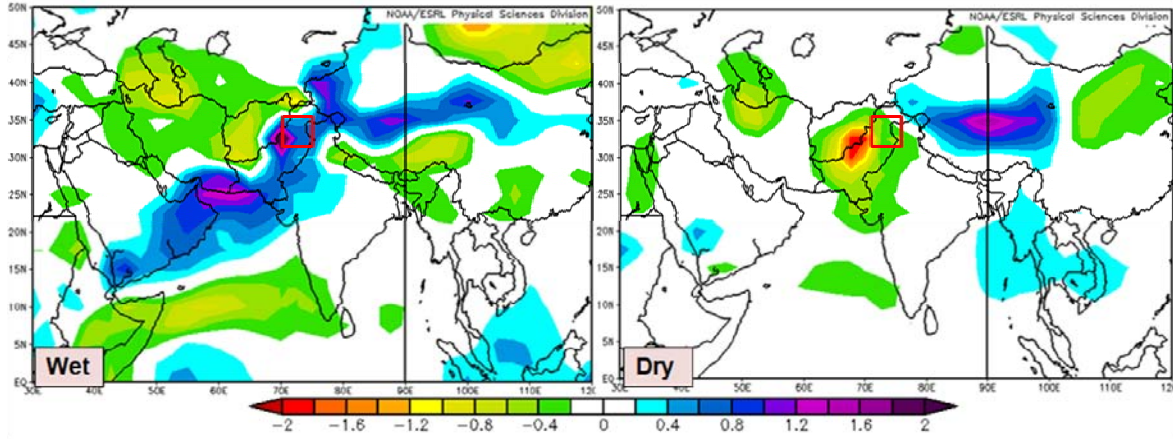


Figure 18. Conditional composite anomalies of 850 hPa specific humidity (g/kg) for the eight most extreme wet (left panel) and dry (right panel) Pakistan PR events during Jul–Aug 1970–2010. The red boxes outline our predictand region.

3. Correlations and Teleconnections

We correlated the time series of Pakistan PR (Figure 11) with several potential predictors from the 1970–2010 period, with the potential predictors leading the predictand by zero to six months at bi-monthly intervals (e.g., Jul–Aug predictand correlated with May–Jun potential predictor). We considered the correlations significant if the coefficient was greater than $+\text{-} 0.30$. The potential predictors included: (a) the MEI, DMI, and NAOI global scale climate variation indices; (b) global SST; (c) global 200 hPa, and (d) global 850 hPa GPH.

One of the primary potential predictors we investigated in our correlation analyses was SST. SST is often a good predictor in LRF systems because:

- (a) Climate variations in the ocean tend to be relatively persistent.
- (b) Relatively small changes in SST can greatly influence climate variations in the atmosphere.

(c) SST variations in one location can significantly impact atmospheric and oceanic conditions in very distant locations via teleconnections.

(d) SST data is readily available in near real time. (van den Dool 2007, Murphree 2010c)

However, as expected based on Figure 15 results, the direct correlation of Pakistan PR with SST at all lead times indicated relatively low correlation values. We correlated Pakistan PR with the MEI, DMI, and NAOI climate variation indices, at bi-monthly intervals with the climate variation indices leading by zero to six months. For all correlations of Pakistan PR versus the three climate variation indices, only the DMI at four to six month leads gave significant correlations, and only marginally. We also correlated Pakistan PR with global SST for the same lead times, and found marginally significant correlations in the eastern Indian Ocean (IO) at two to four month lead times, roughly consistent with the correlations of Pakistan PR with the DMI. These weak or marginal correlations led us to set aside the three global scale climate variation indices and SST as potential direct predictors of Pakistan PR.

We found the most significant correlations with 850 hPa GPH at zero lead (Figure 19). Notice the strong positive correlations in and around Nepal, as well as the strong negative correlation in the southern Red Sea. A slight positive correlation near the Caspian Sea was also evident. This strong correlation pattern of Pakistan PR with 850 hPa GPH existed mainly at zero lead. A slight hint of this pattern was found at the one-month lead, but was absent at longer lead times.

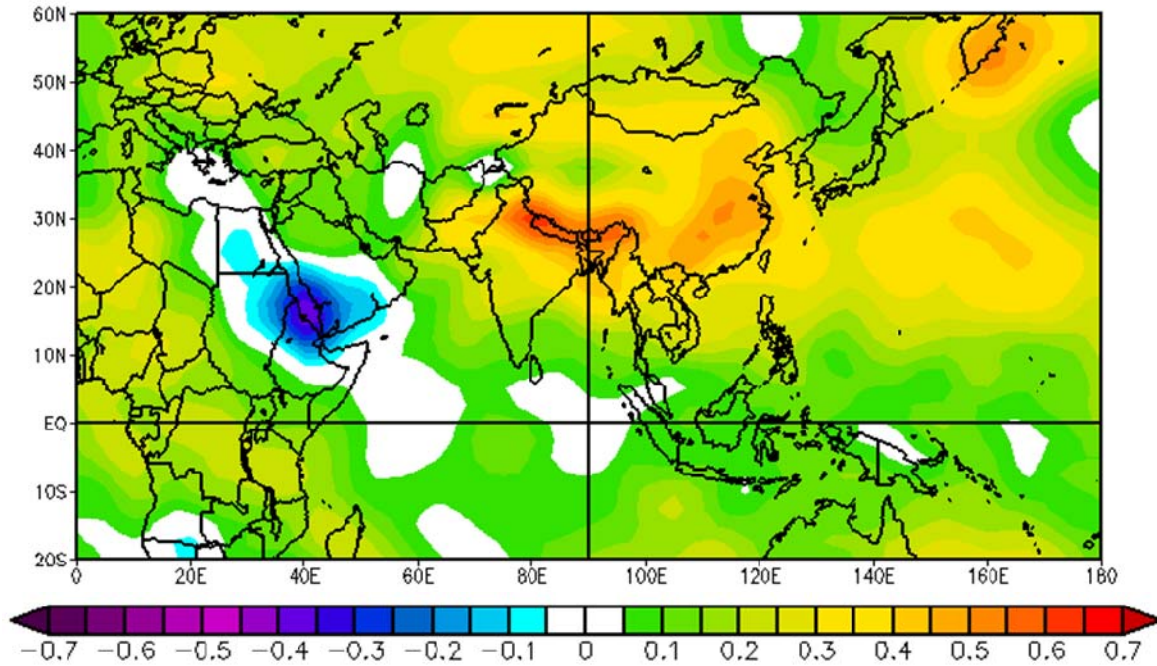


Figure 19. Correlation of Pakistan PR (mm/day) for Jul–Aug 1970–2010 with regional 850 hPa GPH (m) at zero lead. Note the strong positive correlation in the Nepal region, weak positive correlation in the Caspian Sea region, and strong negative correlation in the Red Sea region.

These correlations in Figure 19 are dynamically plausible. For example, in a wet (dry) year, the correlation pattern suggests that the 850 hPa GPH anomalies would be positive (negative) over Nepal, negative (positive) over the Red Sea, and positive (negative) over the Caspian Sea. Consequently, the implied anomalous flow into Pakistan is southerly (northerly) and the implied moisture advection anomaly into Pakistan would be positive (negative), consistent with the composite circulation and moisture anomaly results, especially the AN composite anomalies (see Figures 16, 18).

We also found a significant teleconnection between AN (BN) convection in the eastern IO and maritime continent (MC) region in May–Jun AN (BN) and both Pakistan PR and Nepal 850 hPa GPH in the following Jul–Aug (a two month lead correlation; not shown). These correlations are consistent with our earlier assessment of marginal correlation of Pakistan PR and SST in the eastern IO,

because AN (BN) SST tends to lead to AN (BN) convection in the overlying atmosphere in May-Jun, which then forces AN (BN) lower tropospheric heights near Nepal in Jul-Aug leading to AN (BN) Pakistan PR in Jul-Aug.

Figure 20 schematically represents these physical patterns and processes for wet and dry years.

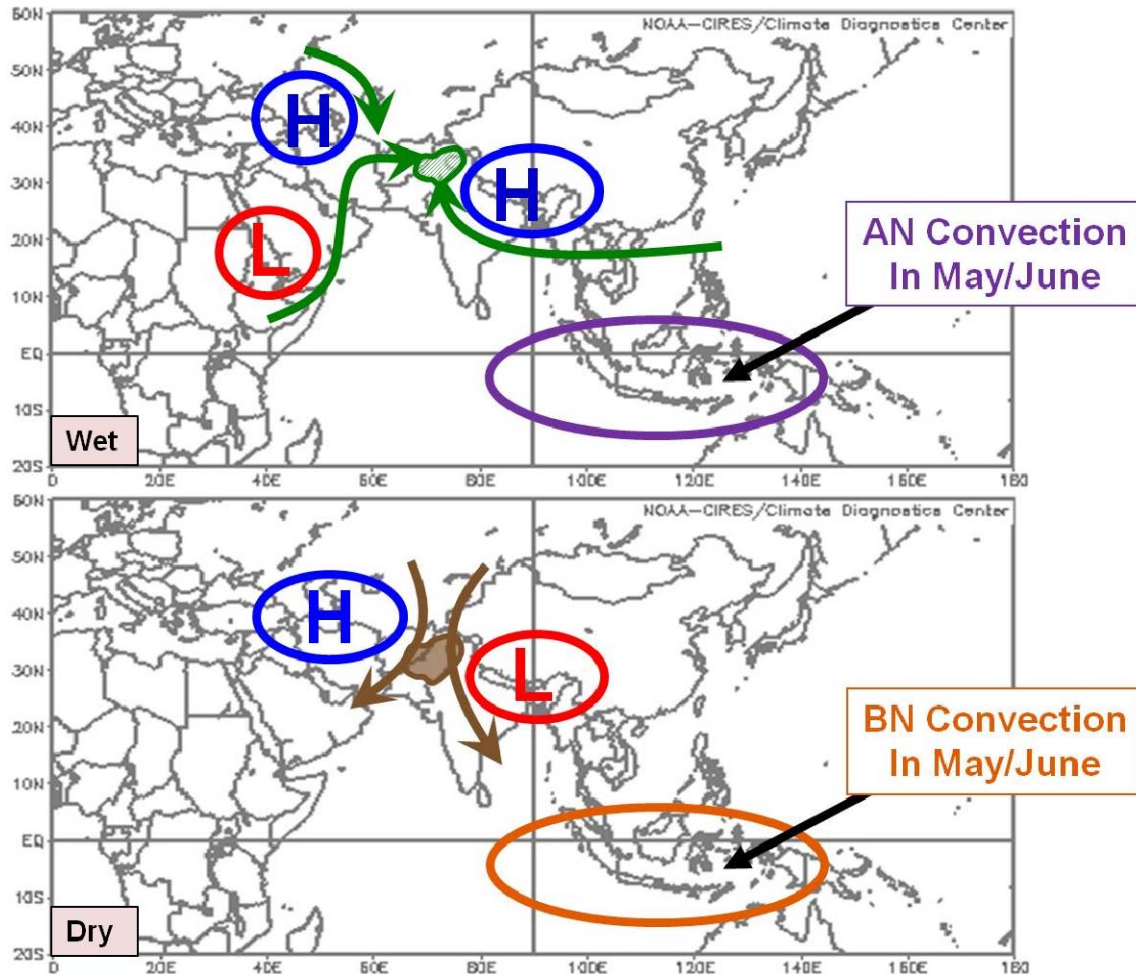


Figure 20. Schematic of 850 hPa GPH anomalies and OLR anomalies for extreme wet (top panel) and dry (lower panel) Pakistan PR events during Jul–Aug 1970–2010. Note during wet (dry) years, the teleconnection of AN (BN) convection near the maritime continent in May–June with higher (lower) tropospheric heights near Nepal in Jul–Aug, indicating a two-month lead teleconnection. Figures based on conditional composite anomaly and correlation results (cf. Figures 14–19).

4. Predictor Selection

a. *Initial Predictors*

Based on our correlation results, we identified 850 hPa GPH in the Nepal, Red Sea, and Caspian Sea regions as potential predictors. We further investigated the viability of these potential predictors by narrowing down our predictor regions. Figure 21a shows the zero lead correlation of Pakistan PR with 850 hPa GPH for Jul-Aug 1970–2010, while Figure 21b is the same correlation for Jul-Aug 2000–2010. We chose our 850 hPa GPH predictor regions based mainly on a combination of the strongest correlations from each of these figures (outlined by the red boxes in Figure 21). Note the strength of the correlations in the Red Sea, Nepal West, and Nepal East boxes in the left panel. In the right panel, a stronger correlation appears in the Nepal boxes as well as the Caspian box and the Afghan box, while the Red Sea box's significance diminishes. The red boxes in Figure 21 account for the most pronounced significant correlations for both: (a) the entire 41-year study period (1970–2010) and (b) the most recent 11-year period (2000–2010). Focusing on the recent 11-year period allowed us to apply the OCN approach of placing emphasis on the trends of the most recent years. See Chapter II, Section B.5.c for a detailed description of the OCN approach. Note too that lower tropospheric GPH anomalies in red boxes could, with the right signs and in combination with each other, lead to circulation and moisture advection anomalies that could produce PR anomalies in the Pakistan PR predictand region in north central Pakistan (cf. Figures 16–20).

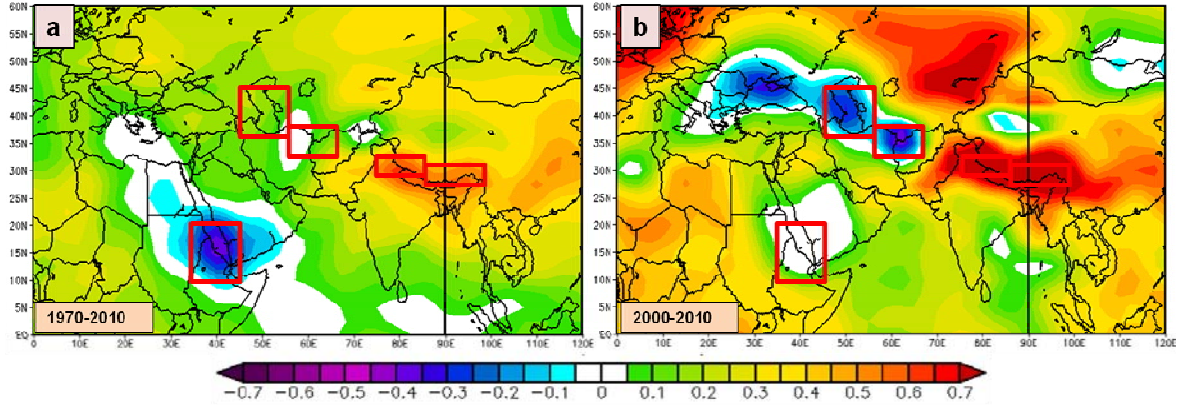


Figure 21. Correlation of Pakistan PR in Jul–Aug with regional 850 hPa GPH for (a) 1970–2010; and (b) 2000–2010. Strong zero lead correlations between Pakistan PR and 850 hPa GPH led to using 850 hPa GPH as our main initial predictor. The red boxes in (a) and/or (b) outline the regions where we observed the strongest correlations. We selected the regions enclosed by these five boxes as our initial predictor regions. These boxes are referred to in this study as (from west to east): Red Sea box (12° – 20° N, 35° – 47° E), Caspian box (35° – 45° N, 45° – 55° E), Afghan box (28° – 33° N, 75° – 85° E), Nepal West box, and Nepal East box (25° – 30° N, 85° – 100° E).

Once our initial predictor regions were selected, we needed to determine the correlation between the predictand and each of the predictors when averaged over their respective regions. Table 3 shows the correlation values for each predictor for the full study period, 1970–2010.

Table 3. Correlation of initial predictors with Jul–Aug 1970–2010 Pakistan PR. Each predictor represents the 850 hPa GPH anomaly within its respective bounded region (Figure 21). The 5-Variable Index denotes a single predictor created by an equal weight combination of all five predictors. Correlations > 0.30 are considered statistically significant at a 95% confidence level.

<i>Predictor</i>	<i>Correlation</i>
Z850 Nepal West Box	0.56
Z850 Nepal East Box	0.54
Z850 Caspian Box	0.16
Z850 Afghan Box	0.07
Z850 Red Sea Box	0.27
5-Variable Index	0.69

Note that only the Nepal West and Nepal East boxes had correlations above our threshold. Yet, when all five predictors were combined to form a single index, we obtained the highest correlation coefficient. This suggested the possibility that each predictor may be useful in predicting Pakistan PR. To determine precisely how much skill, we needed to test the predictors via linear regression. The linear regression results are shown in Chapter III, Section B.1.

b. Final Predictors and Pakistan Summer Precipitation Index (PSPI)

The linear regression results allowed us to optimize our predictor set by eliminating the excess predictors (see Chapter III, Section B.1). Based on these results, we selected 850 hPa GPH in the Nepal West box and the Red Sea box as our final zero lead predictor regions. We combined these two variables to develop a single zero lead predictor index for analyzing and forecasting Pakistan PR in Jul–Aug, which we named the *Pakistan Summer Precipitation Index (PSPI)*. We assigned a weight to each variable in the PSPI, equal to its linear regression coefficient. The formula for the PSPI is:

$$PSPI = (0.07 \times \text{Nepal West 850 hPa GPH Anomaly})$$

$$+ (-0.07 \times \text{Red Sea 850 hPa GPH Anomaly})$$

The units of the PSPI are meters. Figure 22 shows in red the regions for the two PSPI variables.

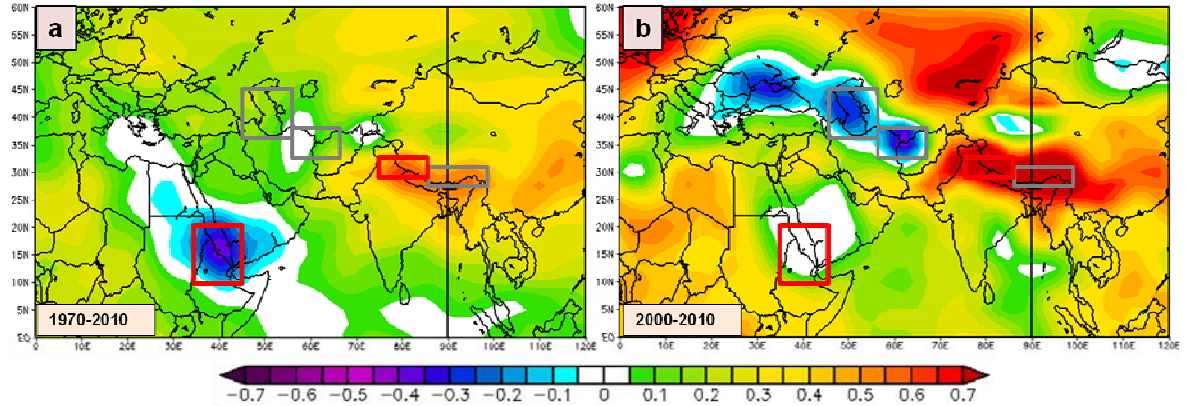


Figure 22. Correlation of Pakistan PR in Jul–Aug with global 850 hPa GPH for (a) 1970–2010; and (b) 2000–2010. This is a duplicate of Figure 21 but with the 850 hPa GPH regions used in the Pakistan Summer Precipitation Index (PSPI) outlined in red and the eliminated predictor regions outlined in gray. The red boxes are the Red Sea box and the Nepal West box (see latitude and longitude ranges in Figure 21).

5. Predictor and Predictand Time Series

Figure 23 compares the time series of our predictor (PSPI) and our predictand (Pakistan PR). With a correlation of 0.694, the relationship is statistically significant at a >99% confidence level. The PSPI correctly represents many of the interannual variations in the Pakistan PR, as well as the overall upward trend in the Pakistan PR (although with some notable exceptions for 1973, 1985–1986, 1998, and 2000–2001). These results indicate that the PSPI has potential as a zero lead predictor of Pakistan PR.

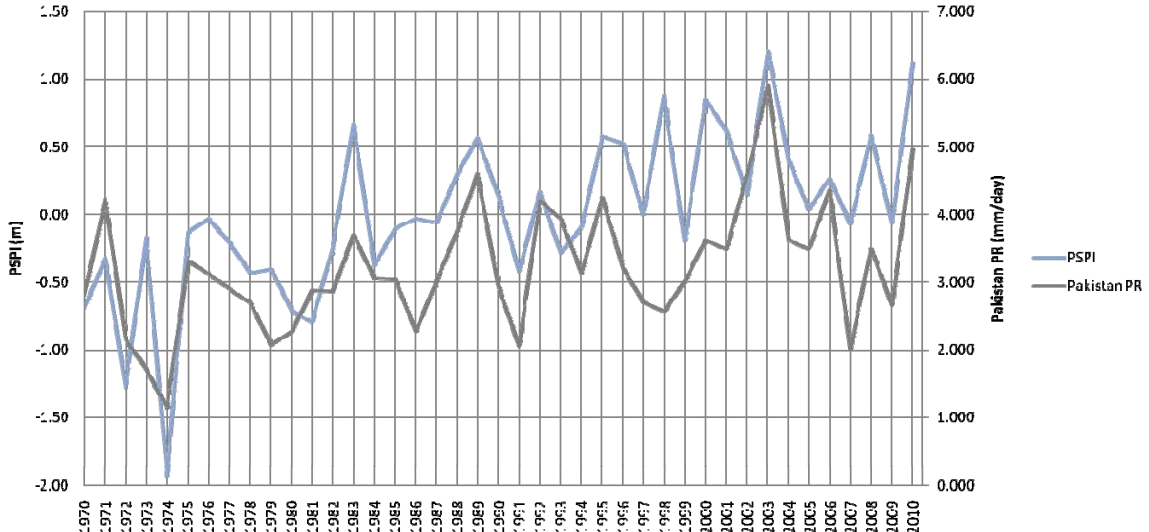


Figure 23. Time series of 1970–2010 Jul–Aug Pakistan PR as observed (mm/day; gray line) and as modeled by the Pakistan Summer Precipitation Index (PSPI, m; blue line). The correlation between the two time series is 0.694, which is statistically significant at a $> 99\%$ confidence level. Note that the PSPI provides a good representation of many of the interannual variations, and of the long-term upward trend, in the Pakistan PR. These results indicate that the PSPI is a high potential to be a skillful zero lead predictor of Pakistan PR.

B. LONG-RANGE HINDCAST RESULTS

1. Linear Regression

We tested the predictors listed in Table 3 via a series of multivariate linear regression models to assess the significance of the predictors in forecasting Jul–Aug Pakistan PR at zero lead. The results of that test are summarized in Table 4. The multivariate results show a very strong relationship between the multivariate index (i.e., an equal weight combination of all five individual predictors) and Jul–Aug Pakistan PR. However, the p-values for the individual predictors show relationships that do not meet our threshold of $p\text{-values} \leq 0.05$ for significance at a 95% confidence level, except for the Red Sea predictor. This indicated that while the multivariate predictor has skill in predicting Pakistan PR, some of the variables within this index overlap with each other.

Table 4. Multivariate linear regression results for our initial predictors (see Table 3) used to model Jul–Aug 1970–2010 Pakistan PR. Each predictor represents the 850 hPa GPH anomaly (Z850) within the regions shown in Figure 21. The multivariate index denotes a single predictor created by an equal weight combination of all five individual predictors. Correlations ≥ 0.30 , significance $F \leq 0.05$, and p-values ≤ 0.05 are considered statistically significant at a 95% confidence level.

<i>Predictor</i>	<i>Correlation</i>	<i>Adj R-Square</i>	<i>Significance F</i>
Multivariate Index (All 5)	0.72	0.45	7.67E-05
			<i>P-Values</i>
Z850 Nepal West Box			0.18
Z850 Nepal East Box			0.58
Z850 Caspian Box			0.43
Z850 Afghan Box			0.22
Z850 Red Sea Box			0.04

To address this overlap problem, we conducted another multivariate linear regression to identify and eliminate the excess predictors. We developed a series of additional multivariate regression models using all possible combinations of the five individual predictors. We initiated these tests of the predictors by including all five original predictors, and then eliminated predictors one at a time. The final round of regression tested only two predictors. We took the additional step of combining predictors that were in close proximity to each other geographically, in other words, we combined the: (a) Nepal West and Nepal East boxes to form the Nepal combination box; and (b) Caspian and Afghan boxes to create the Caspian combination box. We then ranked each of the resulting multivariate regression models according to its adjusted R-square value. As discussed in Chapter II, Section B.5.a, adjusted R-square is a preferred metric to use in multivariate regression as it imposes a penalty for each added predictor (e.g., R-square only increases if the additional variable improves the model more than would be expected by chance), and is utilized to prevent overfitting. The three most significant results from this round of multivariate

regression tests are summarized in Table 5. The results in Table 5 are listed in order of their adjusted R-square values. Note that Table 5.1 and 5.2 have predictors with p-values well over our threshold of 0.05. The predictors in Table 5.3 (outlined in red) had a relatively high adjusted R-square and p-values ≤ 0.05 . For this reason, we selected the Nepal West and the Red Sea regions as our main predictors of Pakistan PR. To do so, we developed an index based on these two predictors with weightings for each predictor equal to its regression coefficient: (a) 0.07 for the Nepal West box; and (b) -0.07 for the Red Sea box. The formula for the resulting index, the Pakistan Summer Precipitation Index (PSPI) is shown in Chapter III, Section A.3.b.

Table 5. The three most significant multivariate regression results, ranked by adjusted R-square, for modeling of Jul–Aug 1970–2010 Pakistan PR. Each predictor represents the 850 hPa GPH anomaly (Z850) within the regions shown in Figure 21. Each of the three multivariate indices denotes a single predictor created by combining the predictors shown just below each of the indices. Correlations ≥ 0.30 , significance $F \leq 0.05$, and p-values ≤ 0.05 are considered statistically significant at a 95% confidence level. The red outline denotes the only multivariate regression model that met each of these thresholds.

1)	<i>Predictor</i>	<i>Correlation</i>	<i>Adj R-Square</i>	<i>Significance F</i>
	Multivariate Index (3)	0.71	0.47	7.86E-06
				<i>P-Values</i>
	Z850 Nepal West Box			2.30E-06
	Z850 Afghan Box			0.19
	Z850 Red Sea Box			0.004

2)	<i>Predictor</i>	<i>Correlation</i>	<i>Adj R-Square</i>	<i>Significance F</i>
	Multivariate Index (4)	0.72	0.46	2.46E-05
				<i>P-Values</i>
	Z850 Nepal Combo			2.83E-06
	Z850 Caspian Box			0.25
	Z850 Afghan Box			0.11
	Z850 Red Sea Box			0.04

3)	<i>Predictor</i>	<i>Correlation</i>	<i>Adj R-Square</i>	<i>Significance F</i>
	Multivariate Index (2)	0.69	0.46	3.69E-06
				<i>P-Values</i>
	Z850 Nepal West Box			2.27E-06
	Z850 Red Sea Box			0.001

2. Tercile Matching

We used the PSPI predictor to generate tercile matching hindcasts of 1970–2010 Jul-Aug Pakistan PR at zero lead. Table 6 and Table 7 show the results of the tercile matching method. Refer to Chapter II, Section B.5.b for further details on this method. See Table 7 for an explanation of the thresholds we set for tercile categories. All values that fell directly on a tercile threshold were rounded to the nearest second order decimal position. See Chapter III, Section B.3 for calculations of the hindcast verification results. Green indicates AN PR, white indicates NN PR, and red indicates BN PR. Note that a correct hindcast for an individual year is indicated by matching colors in the two right columns for that year. Note that BN (AN) hindcasts and observations are most common during the early (later) part of the study period, consistent with the results shown in Figure 11. Note, too, that color matches are common throughout the study period, and especially in the early and later parts of the study period, consistent with the results shown in Figure 23.

Table 6. Tercile matching hindcast results when using PSPI (modeled PR index) to hindcast Pakistan PR (observed PR, mm/day), sorted by year. The years are shown in the left column and the PSPI and Pakistan PR values are shown in the two right columns. Green=AN, white=NN, red=BN. A color match between the two right columns indicates a correct hindcast.

	PSPI	Pak PR
1970	-0.69	2.82
1971	-0.32	4.22
1972	-1.28	2.16
1973	-0.17	1.70
1974	-1.94	1.14
1975	-0.13	3.32
1976	-0.03	3.12
1977	-0.21	2.90
1978	-0.43	2.70
1979	-0.40	2.07
1980	-0.71	2.28
1981	-0.79	2.87
1982	-0.25	2.86
1983	0.67	3.70
1984	-0.37	3.05
1985	-0.10	3.05
1986	-0.03	2.27
1987	-0.06	3.03
1988	0.30	3.77
1989	0.57	4.60
1990	0.13	2.93
1991	-0.42	2.06
1992	0.17	4.20
1993	-0.28	3.94
1994	-0.09	3.14
1995	0.58	4.26
1996	0.52	3.20
1997	0.00	2.71
1998	0.87	2.57
1999	-0.19	3.01
2000	0.85	3.62
2001	0.62	3.50
2002	0.15	4.58
2003	1.20	5.92
2004	0.40	3.62
2005	0.04	3.48
2006	0.27	4.36
2007	-0.07	2.01
2008	0.58	3.50
2009	-0.06	2.66
2010	1.12	4.97

Table 7. Tercile ranges for the results in Table 6. The tercile thresholds were selected by separating the PSPI and Pakistan PR data into thirds. Values in the highest third (middle third, lowest third) were placed in the AN (NN, BN) category.

<i>PSPI Terciles</i>		<i>Observed Pak PR Terciles</i>	
> 0.17	Above Normal	> 3.5	Above Normal
-.17 to .17	Normal	2.87 to 3.5	Normal
< -0.17	Below Normal	< 2.87	Below Normal

3. Hindcast Verification Results

Table 8 summarizes the hindcast verification results for the zero lead tercile matching hindcasts using PSPI to predict Pakistan PR. The overall hindcast verification metrics shown to the right of each sub-table in Table 8 indicated good skill, especially for the hindcasts of AN conditions. For example, HSS is > 0.4 for all categories and > 0.7 for the AN category. The lower performance for the NN category is typical of many LRF systems, as these systems generally are designed to forecast deviations from the NN category (i.e., deviations from LTM conditions). The high skill of the AN hindcasts is especially encouraging since AN PR has the potential to create the most adverse effects (e.g., rapid onset of extreme flooding). Overall, the hindcasts met our performance criteria (i.e., accuracy $> 50\%$, POD $>$ FAR, HSS ≥ 0.3). Given these results, we concluded that the PSPI is a skillful zero lead predictor of Pakistan PR.

Table 8. Contingency table hindcast verification results for tercile matching hindcasts using PSPI to hindcast Jul–Aug 1970–2010 Pakistan PR. The upper (middle, lower) sub-table represents the verification results for the AN (NN, BN) hindcasts. Four verification scores are shown to the right of each sub-table. See Chapter II, Section 5.3 and Table 2 for more information about contingency table-based verification methods.

AN

	obs Y	obs N		<i>Accuracy</i> = 88%
pred Y	12	2	14	<i>POD</i> = .80
pred N	3	24	27	<i>FAR</i> = .08
	15	26	41	<i>HSS</i> = .73

NN

	obs Y	obs N		<i>Accuracy</i> = 76%
pred Y	7	6	13	<i>POD</i> = .64
pred N	4	24	28	<i>FAR</i> = .20
	11	30	41	<i>HSS</i> = .41

BN

	obs Y	obs N		<i>Accuracy</i> = 73%
pred Y	9	5	14	<i>POD</i> = .60
pred N	6	21	27	<i>FAR</i> = .19
	15	26	41	<i>HSS</i> = .41

4. Optimal Climate Normals

As noted in Chapter III, Section A.4, we selected our initial predictor regions based on correlation maps of Pakistan PR with 850 hPa GPH for both: (a) 1970–2010; and (b) 2000–2010. By considering the second of these periods when choosing our predictor, we took into account the OCN approach of placing emphasis on the trends of the most recent years.

Figure 21 shows how correlations of Pakistan PR with 850 hPa GPH have changed during the study period, 1970–2010. In particular, Figure 21 shows that

in the most recent 11 years Pakistan PR and 850 hPa GPH in: (a) the Red Sea region have become less correlated; and (b) the Caspian and Afghan region have become more correlated. This is likely due at least partially to generally higher 850 hPa GPH values across the much of west Asia (e.g., the Caspian Sea region) during 2000–2010 (see Figure 24).

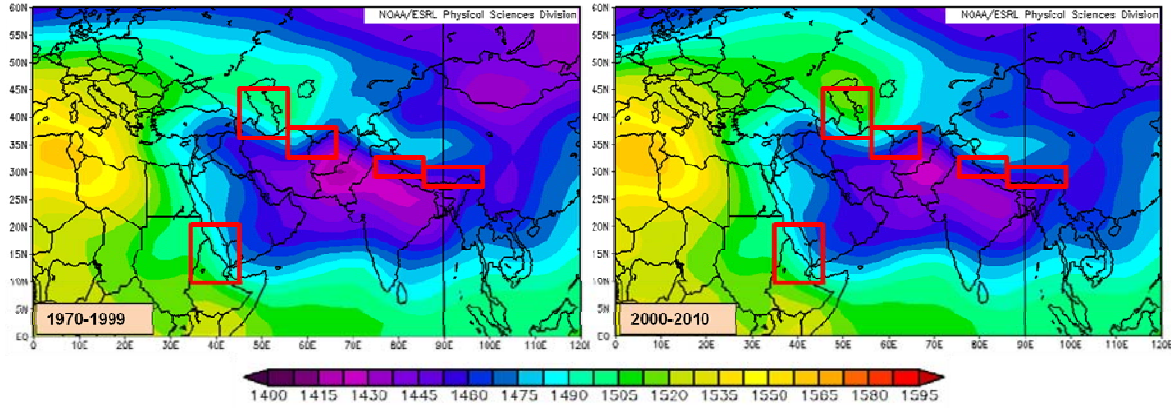


Figure 24. Mean 850 hPa GPH (m) for Jul–Aug 1970–1999 (left panel) and 2000–2010 (right panel). The red boxes represent the boundaries of our initial predictors (see Chapter III, Section A.4.a). Note that mean 850 hPa GPH was relatively high across much of west Asia (e.g., near the Caspian Sea) during 2000–2010. This could be a cause of the changing correlation pattern between Pakistan PR and 850 hPa GPH when comparing the same periods (see Figure 21).

Figure 11 showed the long-term uptrend in Pakistan PR during 1970–2010, and that four of the top eight (50%) of the highest PR observations during the study period occurred during the last eleven years of the period, 2000–2010. To account for these trend changes and to assess the validity of our predictor for the most recent years, we applied an OCN approach by repeating the regression model development and hindcast testing using data from just 2000–2010.

Table 9 shows our OCN multivariate linear regression results. We found that the PSPI still performed well, but that its variables decreased in significance (e.g., Red Sea predictor p-value increased to 0.14). This indicated that we should investigate other potential predictor combinations. We conducted another set of

multiple regression tests by eliminating variables one at a time, similar to the procedure in Chapter III, Section B.1, and then sorted the results using the same criteria as for the results shown in Table 5.

Table 9 shows the results from this OCN approach. In sub-table 9.a, the PSPI is based on data from just 2000–2010. Note from this sub-table that the Red Sea predictor for the PSPI does not meet our p-value threshold for significance. However, a new multivariate predictor index predictor based on the most significant predictors for 2000–2010 does meet all of our significance thresholds (see sub-table 9.b). The predictors for this new index are the same as for the PSPI, but with the Red Sea predictor replaced by the Caspian and Afghan predictors. These results indicate that for modeling Pakistan PR in Jul-Aug 2000–2010, the Red Sea predictor in the PSPI should be replaced by the Caspian and Afghan predictors. We refer to this new zero lead predictor index as the Updated PSPI (UPSPI).

Table 9. Multivariate regression results for Jul–Aug 2000–2010 Pakistan PR using as a predictor: (a) PSPI; and (b) a second combination of predictors to potentially replace the PSPI. Correlations ≥ 0.55 , significance $F \leq 0.05$, and p-values ≤ 0.05 are considered statistically significant at a 95% confidence level. Note in (a) that when PSPI is based on data from just 2000–2010, the Red Sea predictor has a p-value outside our thresholds. The predictors in (b) had the best regression results in modeling 2000–2010 Pakistan PR.

Predictors vs. 2000-2010 Pakistan PR			
<i>Predictor</i>	<i>Correlation</i>	<i>Adj R-Square</i>	<i>Significance F</i>
PSPI	0.90	0.76	1.44E-03
	<i>P-Values</i>		
Z850 Nepal West Box			4.30E-04
Z850 Red Sea Box			0.14

(b)			
<i>Predictor</i>	<i>Correlation</i>	<i>Adj R-Square</i>	<i>Significance F</i>
New Multivariate Index	0.92	0.78	3.23E-03
	<i>P-Values</i>		
Z850 Nepal West Box			0.001
Z850 Caspian Box			0.09
Z850 Afghan Box			0.07

For the UPSPI, we again assigned a weight to each variable based on its coefficients from the regression analysis:

$$\begin{aligned}
 UPSPI = & (0.19 \times \text{Nepal West 850 hPa GPH Anomaly}) \\
 & + (0.11 \times \text{Caspian 850 hPa GPH Anomaly}) \\
 & + (-0.16 \times \text{Afghan 850 hPa GPH Anomaly})
 \end{aligned}$$

We conducted the same tercile matching hindcasting and hindcast verification tests to assess the viability of the UPSPI as a zero lead predictor of Pakistan PR. Those results are summarized in Table 10. The first item to note is the perfect scores for the AN hindcasts. However, the hindcast skills cores were

much lower for the BN and NN hindcasts. We must point out that this is only an 11-year data set, so a single correct or incorrect forecast can greatly change the results. Overall, Table 10 indicates that the OCN approach increased (decreased) the skill of the AN (NN, BN) hindcasts.

Table 10. Contingency table hindcast verification results for tercile matching hindcasts using UPSPI to hindcast Jul–Aug 2000–2010 Pakistan PR. The upper (middle, lower) sub-table represents the verification results for the AN (NN, BN) hindcasts. Four verification scores are shown to the right of each sub-table. See Chapter II, Section 5.3 and Table 2 for more information about contingency table based verification methods.

AN

	obs Y	obs N	
pred Y	4	0	4
pred N	0	7	7
	4	7	11

Accuracy=100%

POD = 1

FAR = 0

HSS = 1

NN

	obs Y	obs N	
pred Y	1	2	3
pred N	2	6	8
	3	8	11

Accuracy= 64%

POD = .33

FAR = .25

HSS = .08

BN

	obs Y	obs N	
pred Y	2	2	4
pred N	2	5	7
	4	7	11

Accuracy= 64%

POD = .50

FAR = .29

HSS = .21

We also compared the skill of the PSPI and the UPSPI by using each of them to perform zero lead hindcasts of Pakistan PR for: (a) the entire 41-year period; and (b) the most recent 11-year period. We then condensed the results from all our long-range hindcast tests into two tables, one for each time period we tested. These results (shown in Table 11) provide a much clearer understanding of which index is the most skilled in predicting Pakistan PR.

These results can be summarized as follows: (a) the PSPI is a better predictor than the UPSPI for zero lead hindcasts of AN, NN, and BN events during the full 41-year period; (b) the UPSPI (PSPI) is a better zero lead predictor of AN (NN and BN) events during the most recent 11 years. These findings indicate that, overall, the PSPI is a better zero lead predictor than the UPSPI. However, this conclusion should be checked in the future as more data becomes available to update both the PSPI and UPSPI.

Table 11. Verification results for zero lead tercile matching hindcasts using PSPI and UPSPI to hindcast Jul–Aug Pakistan PR for 1970–2010 (left table) and 2000–2010 (right table). The upper (middle, lower) sub-table shows the verification results for the AN (NN, BN) hindcasts. Four verification scores are shown in each sub-table. See Chapter II, Section 5.3 and Table 2 for more information about contingency table based verification methods.

1970-2010		PSPI	Updated PSPI	2000-2010		PSPI	Updated PSPI
<i>Correlation</i>		0.69	0.65	<i>Correlation</i>		0.90	0.92
<i>Adj R-Square</i>		0.47	0.41	<i>Adj R-Square</i>		0.76	0.83
<i>Significance F</i>		4.82E-07	4.64E-06	<i>Significance F</i>		0.001	6.43E-05
AN	<i>Accuracy</i>	88%	68%	AN	<i>Accuracy</i>	64%	100%
	<i>POD</i>	0.80	0.53		<i>POD</i>	0.50	1.00
	<i>FA Rate</i>	0.08	0.23		<i>FA Rate</i>	0.29	0.00
	<i>HSS</i>	0.73	0.31		<i>HSS</i>	0.21	1.00
NN	<i>Accuracy</i>	76%	61%	NN	<i>Accuracy</i>	82%	64%
	<i>POD</i>	0.64	0.36		<i>POD</i>	0.67	0.33
	<i>FA Rate</i>	0.20	0.30		<i>FA Rate</i>	0.13	0.25
	<i>HSS</i>	0.41	0.06		<i>HSS</i>	0.54	0.08
BN	<i>Accuracy</i>	73%	68%	BN	<i>Accuracy</i>	82%	64%
	<i>POD</i>	0.60	0.53		<i>POD</i>	0.75	0.50
	<i>FA Rate</i>	0.19	0.23		<i>FA Rate</i>	0.14	0.29
	<i>HSS</i>	0.41	0.31		<i>HSS</i>	0.61	0.21

C. POTENTIAL LONG-RANGE FORECAST SYSTEMS

Our study focused on developing and testing multivariate linear regression models using lower tropospheric GPH predictors for zero lead hindcasting of Jul–Aug Pakistan PR. This focus was determined mainly by the absence of significant, direct, and physically plausible non-zero lead predictors of Jul–Aug Pakistan PR. The skill of the zero lead models is very encouraging but

additional model development is needed to identify methods for predicting at non-zero leads the GPH predictors in the regression models. In this section, we describe three approaches for developing those methods and a non-zero lead LRF system for Jul-Aug Pakistan PR.

1. Direct Statistical Approach

The first LRF approach that we explored was the direct statistical approach, in which a statistical model would be used to predict the Jul-Aug PSPI at non-zero leads, and then this predicted PSPI would be used to predict Jul-Aug Pakistan PR using the multivariate regression model described in the prior sections. Figure 25a shows a two-month lead correlation of SST with Pakistan PR (PSPI). Note that there is no evidence of a strong, direct, non-zero lead relationship between SST and Jul-Aug Pakistan PR. Similar results are found for leads of 0–6 months. However, Figure 25b shows strong, large scale correlations between SST and the PSPI, with SST leading by two months. Similar strong, large scale correlations are found for leads of 0–10 months (not shown). These results indicate that: (a) SST is not be a skillful direct predictor of Jul-Aug Pakistan PR at any leads; but (b) SST may be a skillful indirect predictor of Jul-Aug Pakistan PR when used in a statistical model to produce non-zero LRFs of the Jul-Aug PSPI, which are then used in a statistical model to produce zero lead LRFs of Jul-Aug Pakistan PR.

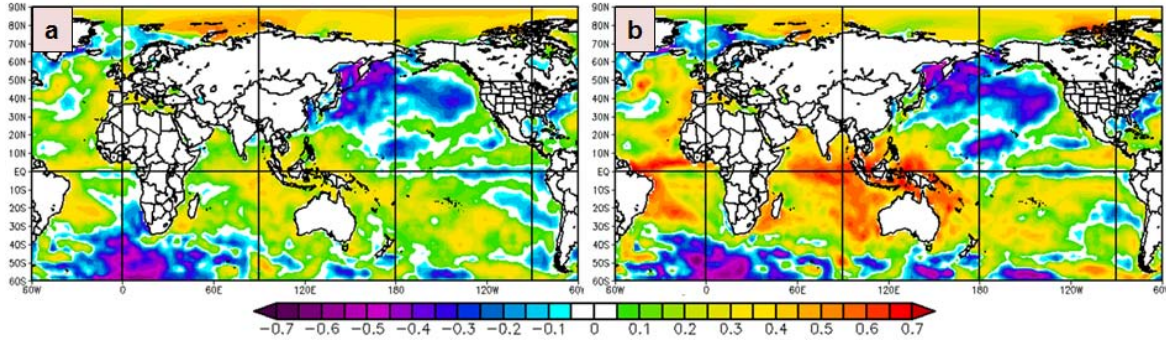


Figure 25. Correlation for 1970–2010 of May-Jun SST with the subsequent Jul-Aug: (a) Pakistan PR; and (b) PSPI (two-month lead correlations). Panel (a) shows a generally weak relationship between SST and Pakistan PR. Panel (b) shows strong relationships between SST and Pakistan PR, and thus indicates a high potential for developing a direct two-step statistical model using SST to produce a non-zero lead forecast of PSPI, and then using this forecasted PSPI to forecast Pakistan PR.

Another intriguing finding was the relationship of SST with the variables used in our PSPI predictor—850 hPa GPH in the Nepal West and the Red Sea regions. Figure 26 shows strong correlations of SST at a two-month lead with these two GPH predictor regions. Figure 26a shows that the Nepal GPH is well correlated with SST in the eastern IO and MC region. Figure 26b shows that the Red Sea GPH is well correlated with SST in the tropical Pacific with patterns that indicate a strong correlation to ENLN variations in SST. These findings provide evidence of the dynamical plausibility of, and potential skill from, using SST as a predictor in a statistical model of Nepal and Red Sea GPH. They also provide indications of the complex and nonlinear relationships between SST, GPH, and Pakistan PR. For example, note the clear differences between the correlation patterns in Figures 26a and 26b. These differences indicate that SST impacts on Jul-Aug Nepal and Red Sea GPH are similar for some ocean regions (e.g., the eastern tropical Pacific) but different for other ocean regions (e.g., the ocean near the MC and in the subtropical western and central Pacific). These similarities and differences are likely to lead to complex nonlinear interactions between SST and the GPH variables that affect Jul-Aug Pakistan PR. These

nonlinearities may help explain why SST is: (a) poorly correlated with Jul-Aug Pakistan PR; but (b) well correlated with the Nepal and Red Sea GPH variables that are well correlated with Jul-Aug Pakistan PR.

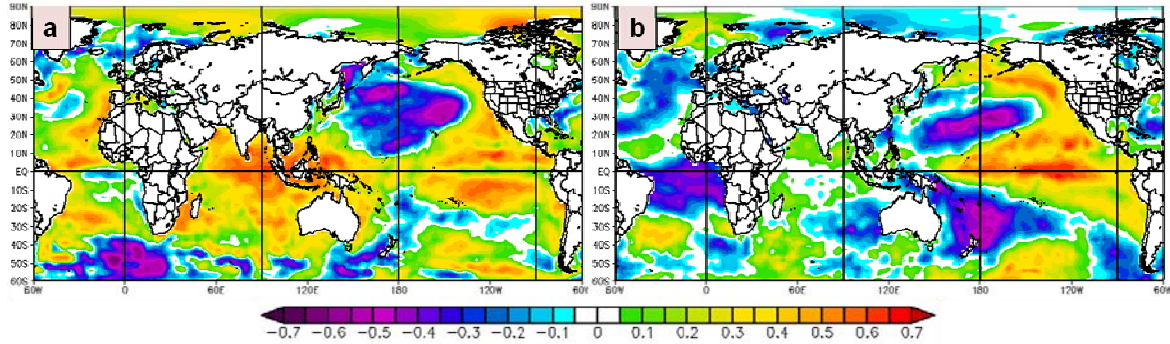


Figure 26. Correlation for 1970–2010 of May-Jun SST with the subsequent Jul-Aug 850 hPa GPH in the: (a) Nepal West region; and (b) Red Sea region (two-month lead correlations). Panels (a) and (b) show strong large scale relationships between SST and the GPH predictor regions. The Nepal GPH appears to have a strong link to SSTs in the tropical IO and MC region. The Red Sea GPH appears to have a strong link to ENLN events in the tropical Pacific. Both figures indicate: (a) the physical plausibility of using global scale SSTs to forecast the 850 hPa GPH variables used in the PSPI; and (b) the potential for using a two-step statistical model to forecast Jul-Aug Pakistan PR.

2. Direct Dynamical Approach

We also investigated the potential for a direct dynamical approach to predicting Jul-Aug Pakistan PR. As the name suggests, this would involve using a dynamical model to directly forecast Pakistan PR, at lead times of, for example, one to six months. An obvious choice for implementing this method would be NOAA's Climate Forecast System (CFS; NCEP 2010, Saha et al. 2006). The CFS is a dynamical modeling system that has demonstrated the ability to produce seasonal forecasts that rival the skill of the statistical methods used by the CPC (Saha et al. 2006). We performed a brief case study of this approach, with representative results shown in Figure 27. This figure shows the two-month lead CFS forecast of PR anomalies for August 2010 PR (left panel) and the

verifying anomalies from R1 (right panel). Note that CFS failed to forecast the extreme AN anomaly in Pakistan and neighboring parts of India that led to record rainfall and flooding in Pakistan. Similar results were found for CFS forecasts of August 2010 PR anomalies at other lead times (not shown). These errors are indicative of the generally low skill of CFS in LRFs of sub-regional PR anomalies (cf. Saha et al, 2006). These results cast doubt on the viability of a direct dynamical LRFs of Jul-Aug Pakistan PR.

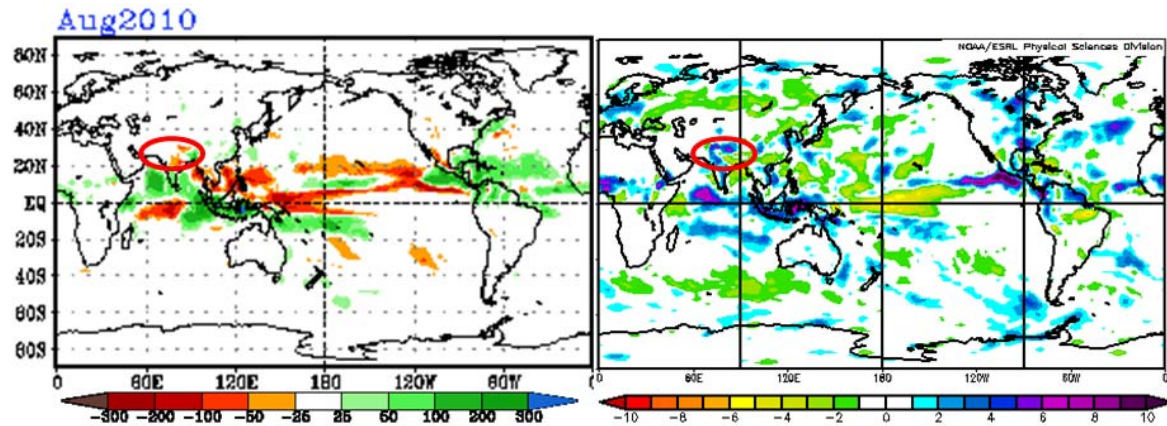


Figure 27. NCEP CFS forecast of Aug 2010 PR at a two-month lead (mm/month, left panel) and verifying NCEP reanalysis of Aug 2010 PR (mm/day, right panel). Note that CFS did not accurately forecast the high PR anomaly over Pakistan.

However, Figure 28 indicates that CFS may have useful skill in forecasting other climate variables related to Jul-Aug Pakistan PR. Figure 28 shows the 700 hPa GPH anomaly for August 2010 from the CFS two-month lead forecast (left panel) and from R1 (right panel). For this case study, we used 700 hPa GPH rather than 850 hPa GPH because the latter is not readily available from NCEP in a graphical format (however, the R1 850 and 700 hPa GPH anomalies are very similar to each other). In this case, CFS correctly forecasted a positive GPH anomaly over south Asia. Similarly, accurate LRFs of 700 hPa GPH were also issued at other lead times out to about six months (not shown). These accurate LRFs are indicative of the relatively good skill of CFS in LRFs of regional scale height anomalies (cf. Saha et al, 2006). These results indicate a

potential for viable LRFs of Jul-Aug Pakistan PR based on a statistical-dynamical approach, as discussed in the following section.

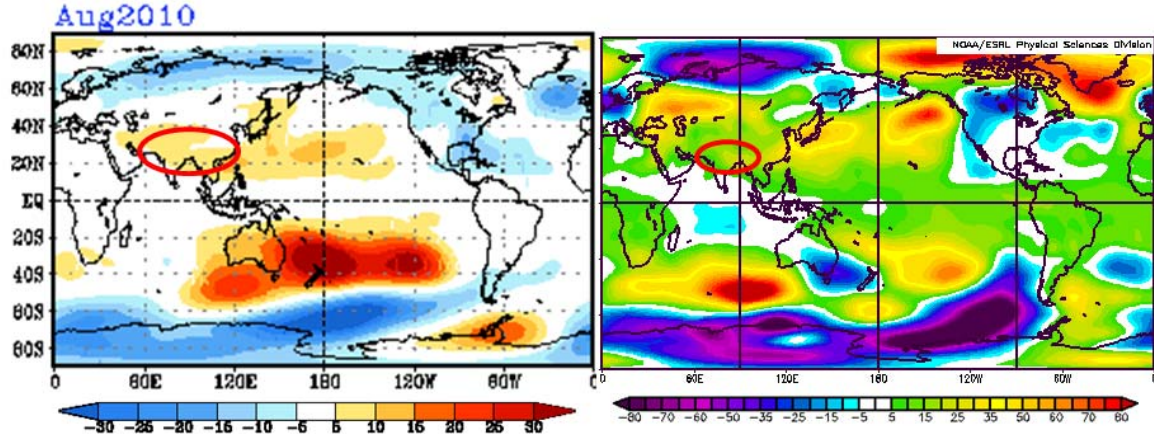


Figure 28. NCEP CFS forecast of Aug 2010 700 hPa GPH at a two-month lead (m, left panel) and verifying NCEP reanalysis of Aug 2010 700 hPa GPH (m, right panel). Note that CFS accurately forecasted the positive GPH anomaly over southern Asia (red oval).

3. Statistical-Dynamical Approach

The third LRF approach we investigated was a statistical-dynamical (S-D) approach. In brief, an S-D approach combines the statistical and dynamical approaches described in the previous two sections. The S-D approach has potential to be the most skillful, as it would exploit the strengths of the statistical and dynamical approaches, and use the strengths of each approach to compensate for the weaknesses of the other method (cf. Mundhenk 2006). For example: (a) the problems that the dynamical approach has in LRFs of sub-regional PR anomalies would be balanced by the skill of the statistical approach in GPH based zero lead forecasts of those anomalies; and (b) the skill of the dynamical approach in LRFs of GPH would compensate for the problems that the statistical approach has with GPH based non-zero lead LRFs of PR anomalies. Figure 29 summarizes the basic methodology behind the S-D approach.

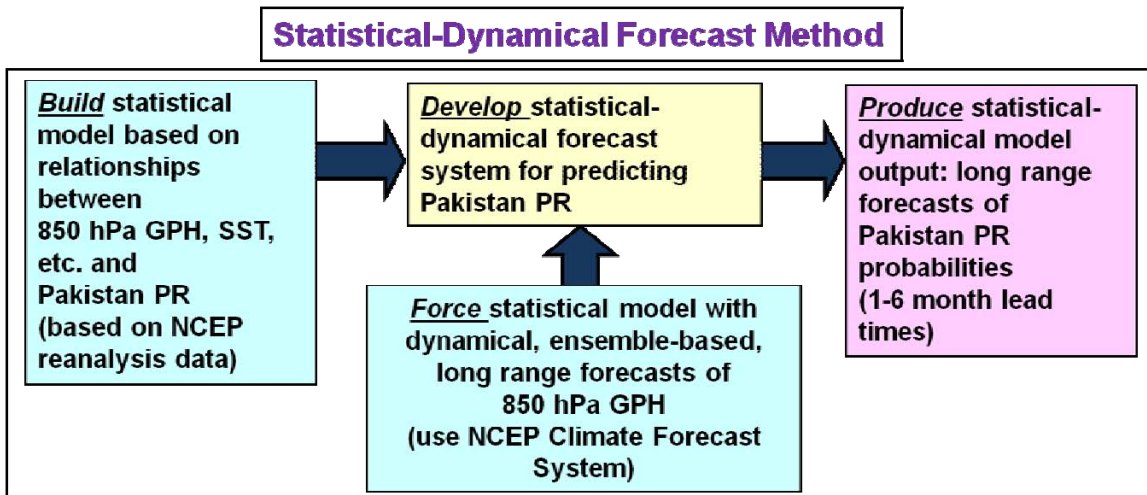


Figure 29. Overview of a statistical-dynamical system for producing LRFs of Jul-Aug Pakistan PR. (After Murphree 2010b)

The basic framework of the S-D approach is to use a dynamical model (e.g., CFS) to produce skillful LRFs of an environmental variable (e.g., 850 hPa GPH) at one to six month leads, and then use those LRFs to force a statistical model that produces zero lead forecasts of the desired predictand (e.g., Pakistan PR). Figure 30 summarizes two potential variations of the S-D approach for producing LRFs of Jul-Aug Pakistan PR. Figure 30a describes the process of: (a) using CFS to forecast 850 hPa GPH (in our PPSI predictor boxes) at lead times of one to six months; then (b) plugging those values into a regression model (i.e., PPSI) at zero lead to forecast Pakistan PR. Figure 30b adds a degree of difficulty by: (a) using CFS to forecast SST at lead times of four to six months; then (b) employing a two-step statistical model in which (1) the predicted SST is used as a predictor in a linear regression model to forecast 850 hPa GPH at lead times of one to three months and (2) the predicted GPHs are used as a predictors in a regression model (i.e., PPSI) at zero lead to forecast Pakistan PR.

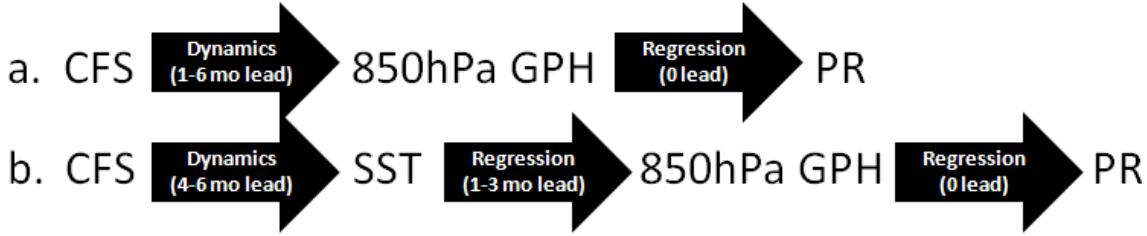


Figure 30. Two potential variations of the S-D approach to producing LRFs of Jul-Aug Pakistan PR. (a) At leads of 1–6 months, use a dynamical model (e.g., CFS) to predict 850 hPa GPH in Jul-Aug, then use the predicted GPH to force a regression model that predict Jul-Aug Pakistan PR. (b) At leads of 4–6 months, use a dynamical model (e.g., CFS) to predict SST at leads of 1–3 months, then use the predicted SST as the predictor in a regression of 850 hPa GPH in Jul-Aug, and then use the predicted GPH in a regression to predict Jul-Aug Pakistan PR.

The S-D approach in Figure 30a has potential because: (a) CFS has already demonstrated relatively good skill in predicting GPH (see previous section); and (b) we have demonstrated statistical skill in using GPH to forecast Pakistan PR via regression in this study. The S-D approach in Figure 30b is more complex and difficult to implement. However, it may be needed if the longer lead LRFs shown in Figure 30a have low skill (e.g., the six month or longer lead LRFs of SST). The Naval Postgraduate School is presently using an S-D model to produce skillful LRFs for tropical cyclone formations in the western North Pacific at lead times out to 90 days and longer, which the CPC is using in its operational products (Mundhenk 2006, Murphree 2010b).

THIS PAGE INTENTIONALLY LEFT BLANK

IV. CONCLUSION AND RECOMMENDATIONS

A. SUMMARY AND KEY RESULTS

This study explored the viability of using advanced climate datasets and methods to skillfully forecast atmospheric conditions at long lead times, in order to enhance the planning processes of both DoD and non-DoD organizations. We stressed the vulnerability and sensitivity that Pakistan has demonstrated to extreme climate events, and the significant threats these events pose to: (a) the political and economic stability of Pakistan; and (b) U.S. national security interests. We chose to focus on Pakistan due to its significance to both: (a) geopolitical and national security affairs; and (b) U.S. military operations.

We specifically investigated the potential for improving long-range forecasts (LRFs) of extreme precipitation events in Pakistan during the summer monsoon (Jul-Aug). Our objectives in this study were to:

1. Understand the physical processes that lead to anomalous summer precipitation events in Pakistan.
2. Develop and test methods for forecasting anomalous summer precipitation events in Pakistan.
3. Develop the basic research foundation for skillful operational LRFs at the intraseasonal and longer lead times needed for effective planning by military and nonmilitary organizations.

Based on the criteria outlined in Chapter I, we chose a customized predictand region within Pakistan for our focus as we developed our long-range forecasting methods for precipitation. We generated composite means and anomalies of a wide range of climate variables to better understand the patterns and processes associated with extreme PR events in Pakistan. We investigated the correlations of these climate variables (e.g., SST and GPH) with Pakistan PR to identify teleconnections that influence anomalous precipitation. We discovered high correlations of 850 hPa GPH with Pakistan PR at zero lead,

indicating the potential skill of this variable as a predictor. We found several regions surrounding Pakistan where 850 hPa GPH showed high correlation with Pakistan PR including the Red Sea, the Caspian Sea, and Nepal. We performed a multivariate linear regression to assess the statistical significance of the potential predictors in each of these regions, and consequently were able to eliminate excess and insignificant predictors. We were left with 850 hPa GPH in specific portions of the Red Sea and Nepal regions as our final predictors. We assigned appropriate weights to each of these predictors based on their respective regression coefficient and combined them in a single index that we classified as our sole predictor of Pakistan PR, which we named the *Pakistan Summer Precipitation Index*, or *PSPI*.

We then performed tercile matching hindcasts and verified those hindcasts to assess the skill of our regression model of the predictor-predictand relationships. We also applied the optimal climate normals (OCN) approach of emphasizing the trends of recent years. Using the OCN method, we discovered a new set of predictors that potentially has better skill for the 2000–2010 period when compared to our results for the entire 1970–2010 study period. We developed another index based on just the 2000–2010 period that we called the *Updated PSPI (UPSPI)*. These are the formulas for the two indices:

$$\begin{aligned} PSPI = & (0.07 \times \text{Nepal West 850 hPa GPH Anomaly}) \\ & + (-0.07 \times \text{Red Sea 850 hPa GPH Anomaly}) \end{aligned}$$

$$\begin{aligned} UPSPI = & (0.19 \times \text{Nepal West 850 hPa GPH Anomaly}) \\ & + (0.11 \times \text{Caspian 850 hPa GPH Anomaly}) \\ & + (-0.16 \times \text{Afghan 850 hPa GPH Anomaly}) \end{aligned}$$

We then repeated our hindcasts and hindcast verification using both PSPI and UPSPI as predictors for 1970–2010 and 2000–2010. We found that the PSPI was the best predictor for 1970–2010, and that the results were mixed for 2000–2010. We concluded that the PSPI is the best choice for forecasting

Pakistan PR, and that more years of data are required to adequately assess the merits of the UPSPI. We found that SST has potential as a predictor of the PSPI at leads of zero to six months.

We concluded the study by providing recommendations on how to incorporate our findings into a forecast system for Pakistan PR. We briefly examined case studies for the forecast approaches that we suggested considering: (a) a direct statistical approach; (b) a direct dynamical approach; and (c) a statistical-dynamical (S-D) approach. We determined that the direct statistical approach and the S-D approach are both physically plausible and have the potential produce skillful LRFs. We determined that the direct dynamical model probably has limited potential for direct LRFs of Jul-Aug Pakistan PR. We expect that further development of these approaches will achieve our final objective of creating timely and accurate LRFs for summer precipitation in Pakistan.

B. RECOMMENDATIONS FOR FUTURE RESEARCH

We have provided compelling evidence that climate analyses and long-range forecasts based on advanced climate datasets and methods can provide immediate and relatively low cost improvements support to both military and nonmilitary planners. This section emphasizes some topics that we recommend be pursued in the near future to ensure that our findings will be implemented into operational LRF processes and operational planning.

1. Conduct further research on the dynamic processes that underlie Pakistan precipitation climate variations. While we developed a basic understanding of the relationships between 850 hPa GPH and Pakistan PR, this is clearly a difficult problem driven by complex dynamical relationships. A better understanding of these relationships will help in developing and testing potential LRF systems.

2. Apply the same LRF data sets and methods to: (a) the other Pakistan precipitation predictand regions; and (b) other potential predictand

variables (e.g., surface temperature and winds); and (c) other potential predictors. Expanding these methods to the other predictand regions will create a better sense of how climate variations affect the whole of Pakistan.

3. Conduct future studies (and/or a repeat of this study) using the updated CFSR and CFS data sets. NOAA has recently introduced upgrades to these products that were not available for the majority our study. The main benefit is that the data is now available in 0.5° resolution as opposed to the 2.5° resolution used for our study.

4. Document correlations of 850 hPa GPH with Jul-Aug Pakistan PR for succeeding years. We highlighted in Chapter III, Section B.4 that our results based on the correlations in 2000–2010 were still inconclusive. If the correlations in the next several years continue to diverge from those for the pre-2000 years, then other predictors may need to be considered.

5. Continue to work toward a skillful non-zero lead LRF system for Pakistan. The statistical and statistical-dynamical approaches we proposed have considerable potential to produce skillful LRFs. We expect that further research and expansion of these approaches will lead to a skillful LRF system for Pakistan in the very near future.

LIST OF REFERENCES

14 Weather Squadron (14 WS), cited 2010: Strategic Climate Information Service. [Available online at <https://notus2.afccc.af.mil/scis/>]

28 Operational Weather Squadron (28 OWS), cited 2010. [available online at: <https://weather.shaw.af.mil/>]

Ahmad, I., 2010: The U.S. Af-Pak strategy: Challenges and opportunities for Pakistan. *Asian Affairs, an American Review*, **37**, no. 4, 191–209.

Air Force Weather Agency (AFWA), cited 2010. [available online at: <http://www.afweather.af.mil/>]

Australian Bureau of Meteorology (BOM), cited 2010. [available online at: <http://www.bom.gov.au/>]

Baker, M., cited 2010: The Coming Conflicts of Climate Change. Council on Foreign Relations. [available online at: <http://www.cfr.org/climate-change/coming-conflicts-climate-change/p22886>]

Barlow, M., M. Wheeler, B. Lyon, and H. Cullen, 2005: Modulation of daily precipitation over Southwest Asia by the Madden-Julian Oscillation. *Mon. Wea. Rev.*, **133**, 3579–3594.

Berger, M., cited 2010: PAKISTAN: PREDICTIONS OF SECURITY THREAT FROM CLIMATE COME TRUE. [available online at: <http://www.proquest.com.libproxy.nps.edu/>]

Climate Prediction Center (CPC), cited 2011. [available online at: <http://www.cpc.ncep.noaa.gov/>]

Cullen, H.M., A. Kaplan, and P.B. deMenocal, 2002: Impact of the North Atlantic Oscillation on Middle Eastern climate and streamflow. *Clim. Change*, **55**, 315–338.

Danielson, E., J. Levin, and E. Abrams, 2003: *Meteorology, 2nd Edition*, McGraw-Hill, 558 pp.

Earth Systems Research Laboratory (ESRL), Physical Sciences Division. cited 2010. [available online at: <http://www.esrl.noaa.gov/psd/>]

European Centre for Medium-Range Weather Forecasts (ECMWF), cited 2011. [available online at: <http://www.ecmwf.int/>]

Financial Post, cited 2010a: Pakistan eyes standing as a 'most climate-vulnerable' nation. [available online at: <http://www.proquest.com.libproxy.nps.edu/>]

—, cited 2010b: Pakistan most vulnerable country to climate change: EU. [available online at: <http://www.proquest.com.libproxy.nps.edu/>]

Gill, A.E., 1980: Some simple solutions for heat induced tropical circulation. *Quart. J. Roy. Meteor. Soc.*, **106**, 447–462.

Global Information Network, cited 2010: PAKISTAN: CLIMATE CHANGE EXPERTS STRUGGLE TO EXPLAIN FLOODS. [available online at: <http://www.proquest.com.libproxy.nps.edu/>]

Hanson, C., 2007: Long-range operational military forecasts for Iraq. M.S. thesis, Dept. of Meteorology, Naval Postgraduate School, 59 pp.

Heidt, S., 2009: Long-range atmosphere-ocean forecasting in support of undersea warfare operations in the western North Pacific. M.S. thesis, Dept. of Meteorology, Naval Postgraduate School, 75 pp.

Hurrell, J.W., NCAR, cited 2006: NAO/NAM Climate Indices. [available online at: <http://www.cgd.ucar.edu/cas/jhurrell/indices.html>]

International Research Institute for Climate and Society (IRI), cited 2011. [available online at: <http://portal.iri.columbia.edu/portal/server.pt>]

Japanese Agency for Marine-Earth Science and Technology (JAMSTEC), cited 2010: Indian Ocean Dipole. [available online at: <http://www.jamstec.go.jp/frsgc/research/d1/iod/>]

Kalnay, E., and Co-Authors, 1996: The NCEP/NCAR 40-year Reanalysis Project, *Bull Amer. Meteor. Soc.*, **77**, 437–471.

Kaufman, S., cited 2010: Pakistan Floods to Factor Highly in Strategic Dialogue with U.S. [available online at: <http://www.america.gov/st/develop-english/2010/October/20101019165234nehpets1.072329e-02.html>]

Kistler, R., and Co-Authors, 2001: The NCEP–NCAR 50-Year Reanalysis: Monthly means CD-ROM and documentation. *Bull. Amer. Meteor. Soc.*, **82**, 247–267.

Kripalani, R., J. Oh, A. Kulkarni, S. Sabade, and H. Chaudhari, 2007: South Asian summer monsoon precipitation variability: Coupled climate model simulations and projections under IPCC AR4. *Theor. Appl. Climatol.*, **90**, no. 3–4, 133–159.

LaJoie, M., 2006: The impact of climate variations on military operations in the Horn of Africa. M.S. thesis, Dept. of Meteorology, Naval Postgraduate School, 153 pp.

Lemke, B., 2010: Long-range forecasting in support of operations in the Horn of Africa. M.S. thesis, Dept. of Meteorology, Naval Postgraduate School, 125 pp.

Mariotti, A., N. Zeng, and K.-M. Lau, 2002: Euro-Mediterranean rainfall and ENLN—a seasonally varying relationship. *Geophys. Res. Lett.*, **29**, 59–1–4.

Matsuno, T., 1966: Quasi-geostrophic motions in the equatorial area. *J. Meteor. Soc. Japan*, **44**, 25–42.

Montgomery, C., 2008: Climate variations in tropical West African rainfall and the implications for military planners. M.S. thesis, Dept. of Meteorology, Naval Postgraduate School, 111 pp.

Moss, S. M., 2007: Long-range operational military forecasts for Afghanistan. M.S. thesis, Dept. of Meteorology, Naval Postgraduate School, 99 pp.

Multivariate ENSO Index (MEI), cited 2010. [available online at: <http://www.esrl.noaa.gov/psd/people/klaus.wolter/MEI/>]

Mundhenk, B., 2009: A Statistical-Dynamical Approach to Intreaseasonal Prediction of Tropical Cyclogenesis in the Western North Pacific. M.S. Thesis, Dept. of Meteorology, Naval Postgraduate School, 107 pp.

Murphree, T., 2010a: *MR3610 Course Module 2: Review of Circulation Patterns and Processes—Part 2*. Dept. of Meteorology, Naval Postgraduate School, Monterey, California, 33 pp.

—, 2010b: *MR3610 Course Module 6: Smart Climatology*. Dept. of Meteorology, Naval Postgraduate School, Monterey, California, 92 pp.

—, 2010c: *MR3610 Course Module 11: Ocean Role in Climate System Part 2*. Dept. of Meteorology, Naval Postgraduate School, Monterey, California

—, 2010d: *MR3610 Course Module 15: Teleconnections*. Dept. of Meteorology, Naval Postgraduate School, Monterey, California, 32 pp.

National Centers for Environmental Prediction (NCEP), Climate Forecast System. cited 2010. [available online at: <http://cfs.ncep.noaa.gov/>]

National Climatic Data Center (NCDC), cited 2011. [available online at: <http://www.ncdc.noaa.gov/oa/ncdc.html>]

National Oceanographic and Atmospheric Administration (NOAA), cited 2011. [available online at: <http://www.noaa.gov/>]

“Pakistan Topography,” Wikipedia, cited 2010. [available online at: http://upload.wikimedia.org/wikipedia/commons/thumb/5/5c/Pakistan_Topography.png]

Ramsaur, D.C., 2009: Climate Analysis and Long-Range Forecasting of Radar Performance in the Western North Pacific. M.S. thesis, Dept. of Meteorology, Naval Postgraduate School, 115 pp.

Saha, S., and Coauthors, 2010: The NCEP Climate Forecast System Reanalysis. *Bull. Amer. Meteor. Soc.*, **91**, 1015–1057. doi: 10.1175/2010BAMS3001.1

—, 2006: The NCEP Climate Forecast System. *J. Climate*, **19**, 3483–3517.

Saji, N. H., B. N. Goswami, P. N. Vinayachandran, and T. Yamagata, 1999: A dipole mode in the tropical Indian Ocean. *Nature*, **401**, 360–363.

State Department Documents / FIND, cited 2010: Background Notes: Pakistan. [available online at: <http://www.proquest.com.libproxy.nps.edu/>]

Stepanek, A., 2006: North Pacific-North American circulation and precipitation anomalies associated with the Madden-Julian Oscillation. M.S. thesis, Dept. of Meteorology, Naval Postgraduate School, 143 pp.

Stone, M., 2010: Long-range forecasting of Arctic sea ice. M.S. thesis, Dept. of Meteorology, Naval Postgraduate School, 91 pp.

Tournay, R., 2008: Long-range forecasting of Korean summer precipitation. M.S. thesis, Dept. of Meteorology, Naval Postgraduate School, 121 pp.

Twigg, K.L., 2007: A smart climatology of evaporation duct height and surface radar propagation in the Indian Ocean. M.S. thesis, Dept. of Meteorology, Naval Postgraduate School, 135 pp.

Turek, A., 2008: Smart Climatology Applications for Undersea Warfare. M.S. thesis, Dept. of Meteorology, Naval Postgraduate School, 95 pp.

U.S. Department of Defense, 2010: Quadrennial Defense Review Report. [available online at: <http://www.defense.gov/qdr/>]

United Kingdom Meteorological Office (UKMO), cited 2011. [available online at: <http://www.metoffice.gov.uk/>]

van den Dool, H., 2007: *Empirical Methods in Short-Term Climate Prediction*. Oxford University Press, 215 pp.

Vastag, B., 2011: Devastating 2010 Pakistan floods highlight difficulties in sounding alarm. *Washington Post*, 14 February. [available online at: <http://www.washingtonpost.com/>]

Vorhees, D., 2006: The impacts of global climate variations on Southwest Asia. M.S. thesis, Dept. of Meteorology, Naval Postgraduate School, 175 pp.

Wilks, D., 2006: *Statistical Methods in the Atmospheric Science*, Academic Press, 627 pp.

THIS PAGE INTENTIONALLY LEFT BLANK

INITIAL DISTRIBUTION LIST

1. Defense Technical Information Center
Ft. Belvoir, Virginia
2. Dudley Knox Library
Naval Postgraduate School
Monterey, California
3. Prof. Tom Murphree
Naval Postgraduate School
Monterey, California
4. Mr. David Meyer
Naval Postgraduate School
Monterey, California
5. Air Force Weather Technical Library
Asheville, North Carolina